Computational Studies of Molecular Interactions Involving Carbon Dioxide and Carbonic Acid

A Thesis submitted in partial fulfillment

for the degree of

MASTER OF SCIENCE

as a part of the

Integrated Ph.D. programme

(Chemical Sciences)

by

Pallabi Haldar

NEW CHEMISTRY UNIT
JAWAHARLAL NEHRU CENTRE FOR ADVANCED SCIENTIFIC RESEARCH
Bangalore – 560 064, India

MARCH 2014

To My Parents,

DECLARATION

I hereby declare that the matter embodied in the thesis entitled "**Computational Studies of Molecular Interactions Involving Carbon Dioxide and Carbonic Acid**" is the result of investigations carried out by me at the New Chemistry Unit, Jawaharlal Nehru Centre for Advanced Scientific Research, Bangalore, India under the supervision of Prof. S. Balasubramanian and that it has not been submitted elsewhere for the award of any degree or diploma.

In keeping with the general practice in reporting scientific observations, due acknowledgement has been made whenever the work described is based on the findings of other investigators. Any omission that might have occurred by oversight or error of judgement is regretted.

Pallabi Haldar

CERTIFICATE

I hereby certify that the matter embodied in this thesis entitled "**Computational Studies of Molecular Interactions Involving Carbon Dioxide and Carbonic Acid**" has been carried out by Ms. Pallabi Haldar at the New Chemistry Unit, Jawaharlal Nehru Centre for Advanced Scientific Research, Bangalore, India under my supervision and that it has not been submitted elsewhere for the award of any degree or diploma.

Prof. S. Balasubramanian
(Research Supervisor)

Acknowledgements

I thank my research supervisor, Prof. S. Balasubramanian for introducing me to the interesting field of computational chemistry. I sincerely acknowledge him for teaching me molecular dynamics simulations and FORTRAN language. I am indebted to him for lending a patient ear to my problems and providing the necessary suggestions and guidance. I am also grateful for the academic freedom that I received in his group and the excellent computing facilities that he has provided for the group.

I am also grateful to our Unit chairman, Prof. C.N.R. Rao for giving me the freedom to pursue my choice of field. Without him, it would never have been possible for me to explore the intriguing field of computational chemistry.

I would also like to thank the faculty members of NCU, CPMU, ICMS and TSU for all the courses they offered. I thank JNCASR for providing excellent research facilities. I acknowledge the Thematic Unit of Excellence on Computational Material Science (TUE-CMS) for providing excellent research ambience.

I am also thankful to the open source community for providing useful softwares and operating systems. In particular, I want to acknowledge the developers of LAMMPS, Gaussian09, CP2K and VMD softwares.

I want to convey my sincere acknowledgements to Dr. Sandeep Kumar Reddy for his help and guidance. I will always be thankful towards him for everything that he has taught me. I am also grateful to all my past and present lab members - Dr. Kanchan Sastri Palla, Rajdeep Singh Payal, B. Satyanarayana, Tarak Karmakar, B.

Karteek, Anirban Mondal, Chaitanya Sharma and Promit Ray for their love, help and guidance. They have come to mean a lot to me.

I want to thank all my friends, seniors and juniors for their love and support. Special thanks to Swastika and Debopreeti for being there for me always. It would not have been possible to do anything without them. Also, I would like to thank Anirban and Neelima for their help and support.

Finally, I would like to thank my family - my mother, father and brother who have loved me and stood by my side everyday for all these years.

Last but not least, I thank everyone who has helped me directly or indirectly.

Preface

The thesis focuses on the computational study of some compounds associated with potential carbon dioxide sequestration pathways. This includes the study on carbonic acid which is involved in the conversion of carbon dioxide to carbonates. Some potential Lewis base - CO_2 interactions are also investigated here. Both classical molecular dynamics simulations and Density Functional Theory(DFT) based calculations have been done for these investigations.

Chapter 1 is a general introduction of global warming and some associated issues. It describes the imminent danger of global warming and its different causes. Carbon dioxide, as a green house gas contributes to it. So, this is followed by a discussion on various carbon dioxide sequestration pathways. Since carbonic acid is involved during the conversion from CO_2 to mineral carbonates, it talks briefly about carbonic acid and its various features. This include the presence of carbonic acid in three different states and its properties like pH. Apart from these, some essential points on classical and ab initio molecular dynamics simulation has also been mooted here.

Chapter 2 explicitly deals with carbonic acid. It mainly talks about the presence of carbonic acid in different forms, its synthesis and associated problems. It highlights the difficulties of studying carbonic acid experimentally and thus focuses on the development of a force field of carbonic acid. This involves some computational calculations and discussions on the conclusions drawn from the same.

In Chapter 3, results from ab initio calculations of some Lewis base and CO_2 have

been discussed. Geometry optimisation have been done for some Lewis base and CO_2 interactions. The optimised structures and the binding energies of the adducts are presented here. Variation of intramolecular properties with change in binding energy are also observed.

Contents

List of Figures

List of Tables

Chapter 1

Introduction

1.1 Carbon dioxide: A problem and the need to sequester it

Nature has her own way of maintaining balance. Carbon cycle is one of such fine balances that maintains total carbon content of the earth by distributing it among the land, oceans and the atmosphere. About two-thirds of the total carbon on earth is permanently stored in fossil fuels, limestone rocks and sediments under the earth. Such reserves of carbon are a result of storage over millions of years, of carbon which was initially present in the atmosphere. Most of the remaining one-third carbon is in relatively long-term storage in the ocean and the earth surface. The forms of carbon in the ocean include dissolved carbon dioxide gas, as carbonates in seashells or in the organic tissues of marine animals. Only a very small part (nearly 1%) of the total carbon content is present in gaseous form in the atmosphere. Most of this carbon is combined with oxygen and resides in the form of CO_2 gas.

Since the onset of Industrial Revolution, fossil fuels - coal,oil and natural gas - have provided the vast majority of energy needed for global industry, business and daily life. All these resources being highly carbon-intensive, the combustion of each of

these involves production of a huge amount of carbon dioxide and its subsequent release into the atmosphere. A large number of forests have been sacrificed to address the needs of the growing population. As a result, humans have released over 300 billion tonnes of carbon once stored in the earth, to the atmosphere in just a span of 150 years.

1.1.1 Greenhouse effect

The sunlight enters the earth after passing through the atmosphere. But when it is being radiated back, some gases in our atmosphere, like carbon dioxide, methane, nitrous oxide trap some of the heat and keeps the earth warm. This is called the GreenHouse Effect(GHE) and the gases involved are called the Green House Gases(GHG). This phenomenon is very important to maintain the temperature of the earth. Without it, the average annual temperature of the earth would be nearly 0 °F which would be too cold for most living beings to survive. GHE ensures that the temperature of the earth is maintained at 59 °F, thus making it the most suitable planet for inhabitation of such diverse lives.[1]

1.1.2 Climate change

But, due to the release of much more carbon dioxide in the atmosphere than that can be sequestered, a severe imbalance has set in the carbon cycle which has resulted in grave consequences. Carbon dioxide being a GHG, its increase in the atmosphere has resulted in the increase in the average temperature on the earth surface. This consequent global warming has led to the melting of ice-caps and glaciers in the poles, change in seasonal cycles and rise in sea-levels. These ominous changes, along with many more, are proving to be detrimental to all forms of life on the earth. The danger is imminent and we need to find a way to prevent this very, very soon.

1.2 Carbon dioxide sequestration

Carbon dioxide sequestration which involves trapping and removal of gaseous carbon dioxide from the atmosphere and storing it into other forms, is one of the best ways to mitigate GHE. There are various ways which have been developed to do this. They include -

1. Biological Sequestration
2. Physical Sequestration
3. Chemical Sequestration

1.2.1 Biological Sequestration

Biosequestration involves carbon sequestration through biological processes which affect the global carbon cycle.

Reforestation

Plants absorb carbon dioxide from the atmosphere and use it for photosynthesis. This removal of atmospheric carbon dioxide can be increased manifold through reforestation. So, forests are often known as 'terrestrial carbon sinks'.[2,3] Four major strategies are available to mitigate carbon dioxide emissions through forestry activities - firstly, increase in the amount of forest cover by bringing more land under forestation. Secondly, increasing the carbon density of existing forests. Thirdly, development and use of forest products to reduce the dependence on fossil fuels and lastly, reducing carbon emissions which occur from deforestation and degradation.[4] There are a number of key points involved in the reforestation issue. Planting trees anywhere on the planet will not have the desired effect. It has been found through extensive research that large reforestation in the arctic or sub-arctic regions will interfere with the reflection of heat from the thick snow cover and thus will not contribute to reduction of global warming. Again, planting trees in the temperate

latitudes would have a net warming effect on atmosphere as the heat released by the leaves is much more than they absorb. So, reforestation in the tropical latitudes can lead to the desired effect through formation of clouds which would reflect the sunlight and reduce the heat. [4,5]

Agriculture

Modification of agricultural practices such that there is a minimisation in the release of carbon dioxide to the atmosphere is one of the potent tools for sequestration. There are two major ways to achieve this - one, practices to reduce emissions of GHG into the atmosphere and two, enhancing carbon removal. Efficient and less energy-intensive agricultural practices like no-till farming not only reduces the release of carbon trapped in the soils but can also act as potential carbon sinks. Decomposition of crops where they lie and subsequent growth of cover crops can reduce GHG emissions and can eventually stop it too.[6] Involvement of agricultural methods that return biomass to soils can help us achieve the second goal. Use of cover crops between planting seasons, restoration of degraded land, increase in the water-retaining capacity of the soils to enhance the growth of carbon-capturing microbes are some of the approaches towards that goal.

Apart from these, some of the other biological sequestration processes are peat production, wetland restoration.

1.2.2 Physical Sequestration

Bio-energy with carbon capture and storage (BECCS)

BECCS[7] exclusively refers to the process of combustion of biomass for energy, the CO_2 emissions from which are captured and stored in geological formations.[8,9] Use of BECCS technology ensures that not only there is no release of CO_2 in the atmosphere, but it is also captured from the atmosphere. So there is a net reduction in

the amount of atmospheric carbon dioxide.

Bio-char

Biochar is a special type of charcoal created by pyrolysis of biomass. It helps to mitigate carbon dioxide emissions by acting as a carbon sink, enhancing negative carbon emissions and also acts as an alternate source of energy.[10] Apart from these, carbon dioxide can be injected into deep ocean or depleted oil and gas reservoirs.

1.2.3 Chemical Sequestration

One of the most widely accepted ways to remove carbon dioxide from the atmosphere is to chemically convert it into some other less harmful chemical species and store it. This process involves carbon dioxide reacting with metal oxides like magnesium oxide or calcium oxide to form stable carbonate minerals.[11,12] Some other processes involved are :

Chemical Scrubbers

These are devices which trap exhaust fumes from industrial plants and treat those gases so as to remove the harmful contents in the fumes. Examples of such scrubbers involve amine scrubbers and activated carbon.[13] Other processes involve injecting carbon dioxide into deep-sea formations. These injected carbon dioxide reacts with the basalt and thus forms stable carbonate minerals.[14,15] Secondly, carbon dioxide forms carbonic acid whenever it dissolves in water. The resulting ocean acidification prevents further absorption of atmospheric carbon dioxide. It is neutralised by adding bases like crushed limestone, sodium hydroxide .[16,17] The changing environment is a warning to the human race to take the necessary actions against the excess carbon dioxide emission and global warming. The above mentioned methods demonstrate that people have started taking serious measures to fight the challenge.

However, we have a long way to go. In this work here, we have addressed one of the methods - converting carbon dioxide into stable carbonate minerals. Some of the species involved in the process are addressed in the subsequent paragraphs.

1.3 Carbonic acid

The interaction of carbon dioxide with water involves an equilibrium which, in turn, leads to the formation of carbonates, bicarbonates and carbonic acid. That equilibrium[18] involved is

$$CO_2 + H_2O \rightleftharpoons H_2CO_3 \rightleftharpoons HCO_3^{-1} + H^+ \rightleftharpoons CO_3^{-2} + 2H^+ \tag{1.1}$$

This reaction takes place almost all the time in different situations. Ocean water is a little acidic. The carbon dioxide imbalance has led to further increase in the ocean acidity. As a result, the acidic water reacts with the carbonate minerals under the sea and results into their subsequent dissolution. Also, the hard outer shells of many sea animals like oysters, sea urchins, deep sea corals are made of carbonate minerals.[19] Such an increase in the acidity of the water leads to a dramatic effect on these shells too . They slowly start to dissolve thereby killing the organisms in the process. The death of such sea animals in large numbers[20] leads to imbalance in the oceanic food chain as well as disastrous effect on the economy of many nations dependent on oceans for various purposes like food and industry.

Secondly, this equilibrium is maintained in our own body.[21] The body maintains a fine balance between carbon dioxide and bicarbonate levels in the blood stream thereby maintaining the body pH at around 7.40 $\pm$ 0.05. Too acidic conditions like (pH <7.35) leads to acidosis whereas too basic conditions like (pH >7.45) leads to alkalosis. Both these conditions lead to serious disorder in the human body. A class of enzyme known by the name of Carbonic Anhydrase helps to maintain this

equilibrium by catalyzing the conversion from carbon dioxide to carbonic acid and vice-versa. In the absence of this catalyst, this reaction is quite slow.

Out of all the species involved in this equilibrium, carbonic acid drew our attention because of its interesting features. Firstly, it is very unstable in aqueous solution (lifetime of a few nanoseconds). So, it was almost impossible to elucidate it from the reaction mixture. People did not believe in its independent existence for a long time until in 1991, when Moore and Khanna[22] succeeded in detecting solid carbonic acid. Later, in 1993, Mayer's group from Innsbruck[23] first isolated solid films of pure carbonic acid. Apart from its presence in all the conditions mentioned above, it is present in inter-planetary spaces, in comets, either in gas phase or as solids. It may also be present in carbonated beverages.

1.3.1 Conformers of Carbonic Acid

Carbonic acid is a diprotic acid with two exchangable protons in aqueous solution. Depending on the relative position of one proton with respect to another, it can be classified into three different conformers - anti-anti conformer, anti-syn conformer and syn-syn conformer. These are the three stable conformers, out of which the most stable is the anti-anti one followed by the anti-syn conformer and then the syn-syn conformer. The reason behind such stability order is the formation of intra-molecular weak hydrogen bonds between the carbonyl oxygen and the hydrogen atoms of the same molecule. For the anti-anti conformer, there are two such hydrogen bonds, for anti-syn conformer, only one such hydrogen bond can be formed whereas for the syn-syn conformer no such bonds could be formed. Hence the stability. Gas-phase calculations at the CBS-QB3 level of theory show that the anti-anti conformer is more stable than the anti-syn conformer by 1.53 kcal/mol energy and from the syn-syn conformer by about 9.85 kcal/mol.[24] These features are illustrated into the diagram below -

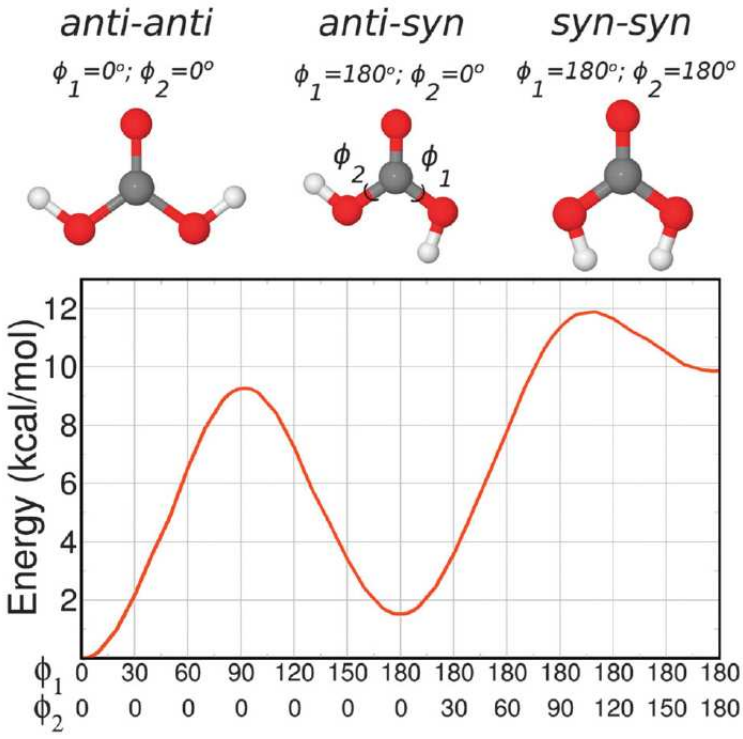

Figure 1.1: Three conformers of carbonic acid located on the potential energy surface drawn as a function of the two dihedral angles. Energies are calculated at the CBS-QB3 level of theory. Reproduced with permission from ref [24]

Carbonic acid also forms stable homodimers. Strong intermolecular hydrogen bonds are responsible for the formation of such dimers. The dimer can be a cyclic six-membered ring formed due to two hydrogen bonds between two monomers. They appear as :

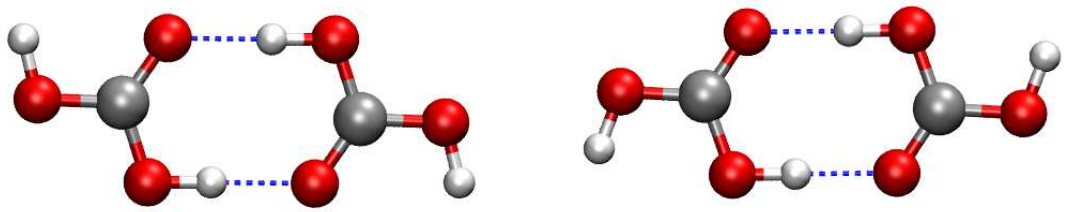

(a) anti-anti dimer **(b)** anti-syn

Figure 1.2: Carbonic acid dimers

Carbonic acid can be present in three different phases - gaseous, aqueous and solid. It shows specific characteristics in each of these phases. Over the years, people have tried to synthesise carbonic acid in all the three phases. So, here, in the following paragraphs, we have roughly summarised earlier studies on carbonic acid.

1.3.2 Gas phase

As recently as 2003, gaseous carbonic acid was first reported by Schwarz and coworkers from the decomposition of NH_4HCO_3.[25] In 2009, for the first time, Mori and coworkers synthesised cis-trans conformer of carbonic acid by applying a pulsed high voltage of 1.8 kV on a sample gas mixture consisting of 5% of CO_2 diluted with Ar. The sample gas mixture was first passed through a reservoir filled with water. Later, microwave spectroscopy was used to detect and confirm the formation of cis-trans conformer of carbonic acid.[26] By employing a similar technique, cis-cis conformer of carbonic acid was synthesised and detected in 2010 by the same group.[27] It had been shown much earlier that solid carbonic acid can be isolated as two distinct polymorphs - the α and the β carbonic acid in laboratory using

cryogenic techniques.[23] α-carbonic acid can be sublimed at 210 K and trapped as carbonic acid monomers and dimers at 6 K. Surprisingly, it was found that when the gaseous carbonic acid was recrystallised back to the same polymorph by evaporating the matrix at 180 K, there was no decomposition of carbonic acid. This was a powerful observation which established the fact that gas-phase carbonic acid is stable and do not decompose to water and carbonic acid, as in aqueous phase.[28] This suggests that carbonic acid may exist in astrophysical environments in gaseous form without decomposition. In extraterrestrial environment like in Mars, in comets like Hale-Bopp, the absence of water and the temperature is conducive to the formation and existence of carbonic acid. Similar investigations were carried out for β-carbonic acid as well. The vapor phase of β-carbonic acid is more difficult to isolate because the vapor pressure and the sublimation rate of this polymorph is lower than that of the α-polymorph. Hence isolation is done at higher temperatures (230-260 K).[29] Interestingly, it was found that the gas-phase β-carbonic acid can also be recrystallised back to the polymorph without decomposition, thus implying that this polymorph is also stable in the gas phase. This makes the earlier hunch about the existence of carbonic acid in extraterrestrial spaces much stronger. It is important to mention at this point that the population ratio of the different type of species in the gas phase shows different trends for the two different polymorphs. For the α-carbonic acid, the ratio of the *anti-syn* monomer to the *anti-anti* monomer to the *anti-anti* hydrogen bonded *dimer* is 1: 10: 1.[30] But, in the case of β-carbonic acid, the *anti-anti dimer* is absent in the gas phase. The probable reason for the absence of dimer in the gas phase might be the increased temperatures which leads to an increase in the entropy, which in turn disfavours dimers over monomers. The ratio of the *anti-anti* monomer to the *anti-syn* monomer in the vapour phase is in between 5 to 10. Upon irradiating with UV, more number of anti-syn conformers are formed from anti-anti conformers.[30]

1.3.3 Aqueous Phase

Aqueous solutions containing dissolved CO_2 and various other carbonate species occur in a variety of natural environments and have major impacts on many processes. There exists an equilibrium as mentioned in eq(1). The species present in such a solution include H_2CO_3(carbonic acid), HCO_3^-(bicarbonate), CO_3^{2-}(carbonates) and dissolved CO_2. The amount of CO_2 converted to carbonic acid is very,very less (nearly 1%).

In 2009, Kumar et al[31] studied the hydrogen-bonding structure and dynamics of aqueous carbonic acid using a system of some water molecules and a single molecule of each different species. They found that the hydration structures of the different carbonate species depend on the type of hydrogen bonds formed between them and water molecules. When C-O-H group of carbonate species are the donor in the hydrogen bond formation, it resulted in the formation of a stronger hydrogen bond than when water O-H is the hydrogen bond donor.Later, in 2014, Reddy et al reported on similar lines that water interacted strongly with the hydroxyl group of carbonic acid than the carbonyl group after performing Born-Oppenheimer Molecular Dynamics Simulations(BOMD) on a bulk system of some water molecules and one molecule of carbonic acid.[24] Pair correlation functions were calculated between different atom types of carbonic acid and water atoms for both the conformers of carbonic acid - the *anti-anti* and the *anti-syn*. The g(r) appears different for the two different conformers. It appears that the anti-syn conformer is a better acceptor of hydrogen bond than anti-anti conformer.

Reaction equilibrium

The reaction equilibrium of carbon dioxide in water is as mentioned in equation (1). Gaseous carbon dioxide dissolves in water to form aqueous carbon dioxide according

to the equation[24] -

$$CO_2 + H_2O \rightleftharpoons CO_2(aq.) \tag{1.2}$$

This dissolved CO_2 forms H_2CO_3 which again dissociates into bicarbonate ion HCO_3^- as -

$$CO_2(aq) \rightleftharpoons H_2CO_3 + CO_2(aq.) \rightleftharpoons HCO_3^- + H^+ \tag{1.3}$$

The apparent dissociation constant for the above reaction is given by K_1 as:

$$K_1 = \frac{[H^+]\left[HCO_3^-\right]}{[CO_2 + H_2CO_3]} \tag{1.4}$$

The actual dissociation constant of carbonic acid, H_2CO_3 is given by the acid dissociation constant, K_a, as:

$$K_a = \frac{[H^+]\left[HCO_3^-\right]}{[H_2CO_3]} \tag{1.5}$$

So, now we have by combining both the dissociation constants as:

$$\frac{K_a}{K_1} = \frac{[CO_2 + H_2CO_3]}{[H_2CO_3]} \tag{1.6}$$

or,

$$K_a = K_1 + \left[1 + \frac{[CO_2]}{[H_2CO_3]}\right] \tag{1.7}$$

The ratio of the concentration of CO_2 to H_2CO_3 is very difficult to calculate due to the very low concentration of H_2CO_3. Hence K_a is calculated indirectly by employing different methods.

pK_a

The concentration of the dissolved CO_2 and carbonic acid was used by Nibbering and coworkers[32] to determin K_a by using ultra-fast spectroscopy during the protonation of HCO_3^- to H_2CO_3. Meyer's group employed a similar protocol and observed the deuteron transfer reaction from DCO_3^- to CA in a deuterated aqueous solution. They successfully detected three different species, namely, carbonic acid, bicarbonate and carbonate by monitoring different bond-stretching infra-red bands.[21] They reported the rate of deuteron transfer from DCO_3^- to CA as 1.7 x 10^{11} s^{-1}. Using this information, they calculated the pK_a of carbonic acid to be 3.45±0.15. This discards the myth of carbonic acid being a weak acid and establishes the fact that carbonic acid is a strong acid.

1.3.4 Solid Phase

Moore and Khanna condensed mixtures of gaseous CO_2 and H_2O which resulted in the formation of thin films, which, in turn, were irradiated with high energy protons to facilitate protonation.[33] The formation of carbonic acid under such conditions were confirmed by the help of IR spectroscopy and mass spectroscopy. Later, Mayer and co-workers synthesised carbonic acid without employing high energy irradiation methods. They succeeded in preparing thin films of crystalline CA. The use of a methanolic bicarbonate solution yielded the α-polymorph while the use of an aqueous one yielded the β-polymorph of carbonic acid. They were identified and differentiated based on their IR vibrational modes and distinct thermal stabilities. Out of many differences in the IR spectra of the two polymorphs, the most prominent one was in the in-plane bending mode of C-OH group - there is a shift of 124 cm^{-1} for the same mode.[34] Even though crystalline thin films of solid carbonic acid have been synthesised, the crystal structures of such films could not be elucidated as yet, thanks to the difficulties in preparation of single crystals and hazy X-ray

powder patterns. However, Mayer's group have been able to observe the phase transition from amorphous to crystalline phase of both the polymorphs of carbonic acid within a temperature range of 200 to 230 K.[35] The most important observation from this study was that the characteristic system properties of each polymorph remain unchanged even after the transition from its crystalline to its amorphous state and vice-versa. The IR spectra bore the proof of such a claim. But, the X-ray diffraction patterns of the amorphous forms of the two polymorphs were found to be different, thus, establishing the fact that the structural features of these two polymorphs are maintained in both the phases - amorphous and crystalline. Lastly, it is important to mention that both polymorphs sublime at and above 200 K, without decomposition, thus establishing the stability of carbonic acid in gas-phase. As, it has been mentioned earlier (refer to gas-phase section), this fact implies the presence of carbonic acid in the extra-terrestrial environment and in the inter-planetary space.[28]

1.4 Molecular dynamics

Molecular dynamics is a numerical technique used to calculate forces acting on the atoms of the system and to propagate the degrees of freedom in time. That force, is nothing but the negative gradient of potential energy with respect to the atom position. MD can be broadly classified into two branches - classical MD and ab initio MD. In classical MD, the potential is a function of the atomic coordinates only, whereas, in ab initio MD, the potential is a function of both the electronic and nuclear coordinates.

1.4.1 Classical Molecular Dynamics

Here, the classical Newton's equation of motion are solved for computing the equilibrium and transport properties of a classical many body system. The classical equations of motion for a simple atomic system are given as -

$$\mathbf{f_i} = m_i \ddot{\mathbf{r}} \tag{1.8}$$

where $\mathbf{f}_i$ is the force acting on i^{th} particle, m_i is the mass of the i^{th} particle and $\ddot{\mathbf{r}}$ denotes the acceleration of the i^{th} particle. The force acting on the i^{th} particle is related to the potential energy of the system, U as -

$$f_i = -\frac{\partial U}{\partial r_i} \tag{1.9}$$

For a system consisting of N particles, the total potential energy of the system is given as $U(r^N)$ where $r^N = (r_1, r_2, ...r_N)$ denotes the 3N coordinates of all the N particles in the system. There are two major contributions to the total potential energy of the system - energy from the bonded interactions (or, intramolecular interactions), U_b and the energy from the non-bonded interactions (or, inter-molecular interactions), U_{nb}.

The intramolecular energy, U_b can be written as a sum of the contributions from bond stretches - U_{bonds}, angle flexing - U_{angles}, torsional rotations - $U_{dihedral}$ and improper interactions - $U_{improper}$. This is given as -

$$U_b = U_{bonds} + U_{angles} + U_{dihedral} + U_{improper} \tag{1.10}$$

The intermolecular energy, U_{nb} is given as the sum of 2-body, 3-body,..., N-body terms as-

$$U_{nb}(r^N) = U_{2body} + U_{3body} + ... + U_{Nbody} \tag{1.11}$$

In most calculations, three-body and higher terms are neglected as they are expensive to calculate. It is only the two-body interaction term, also known as pair-potential, which is considered for most practical purposes. One of the most commonly used pair-potential forms is the Lennard-Jones potential,v^{LJ}, which is written as,

$$v^{LJ} = 4\epsilon \left[\left(\frac{\sigma}{r} \right)^{12} - \left(\frac{\sigma}{r} \right)^{6} \right] \tag{1.12}$$

The Lennard-Jones potential contains two important parameters - σ, the diameter and ϵ, the well depth. r is the pair-wise distance. The electrostatic interactions are calculated using Coulomb potential,$v^{Coulomb}$, as -

$$v^{Coulomb}(r) = \frac{Q_1 Q_2}{4\pi\epsilon_0 r} \tag{1.13}$$

where Q_1, Q_2 are the charges of the two interacting molecules, r is the pair-wise distance and ϵ_0 is the electrical permittivity of the space.

Force-field is a description of the potential energy of the system, containing the values of the set of bonded and non-bonded parameters to perform MD on the system. Hence, this is used to calculate the forces on the system using that specific potential form.

1.4.2 Ab initio Molecular Dynamics

There are certain drawbacks of classical Molecular Dynamics which limit its applications. The major limitation is that the results are dependent on the extent of perfection of the model used. The more perfect the model, the more perfect is the description of the system. But, determining a new potential form for a new complex system with many interactions is a challenging task. Another problem is the transferability of such potentials. Ab initio molecular dynamics deals with the calculation of electronic degrees of freedom. This method exploits the Born-Oppenheimer

approximation that solves the electronic Schrödinger equation for a given nuclear configuration. Analogous to Classical Molecular Dynamics where the forces on each particle are calculated by solving Newton's equations of motion, here, at first, the electronic distribution in the ground state is determined from the Schrödinger's equation after which, the forces are calculated by using Hellmann-Feynman theorem.

According to Bloch's theorem, each electronic wave function can be expressed as a sum of plane waves as -

$$\psi_i = \sum_k C_k^i e^{veck,vecr} \tag{1.14}$$

where the coefficients of expansion are $C_k{}^i$'s. The electronic wavefunction can be expressed by a complete set of coefficients, denoted by C. Thus, it can be seen that for condensed phases, the wave-function consists of two parts - a periodic part and a phase factor. The periodic part is expressed by plane waves basis-sets.

Density Functional Theory

Another important concept widely used in ab initio Molecular Dynamics is Density Functional Theory. This theory essentially relies on two theorems - the Hohenberg-Kohn Theorems. The first theorem expresses the ground-state wavefunction as a function of the ground-state electron density, as -

$$\psi_0 (r_1, r_2, ...r_N) = \psi [n_0 (r)] \tag{1.15}$$

Here,ψ_0(r) represents the ground state wavefunction and n_0(r) represents the ground state electron density. So, it directly follows from this, expectation value of any ground state observable $\hat{O}$ is a functional of ground state electron density n_0(r),as -

$$O_0 = O[n_0] = \langle \psi[n_0|\hat{O}|\psi[n_0] \rangle \tag{1.16}$$

The second theorem deals with the calculation of ground state energy. This energy is expressed as -

$$E_{v,0} = E_v[n_0] = \langle \psi[n_0] | \hat{H} | \psi[n_0] \rangle \tag{1.17}$$

where the total Hamiltonian is expressed as a sum of Kinetic energy(T) and Potential Energy(U+V) as $\hat{\mathrm{H}} = \hat{\mathrm{T}} + \hat{\mathrm{U}} + \hat{\mathrm{V}}$. Similar to the variational theorem, the ground state energy has the variational property, as

$$E_v[n_0] \leq E_v[n^{'}] \tag{1.18}$$

This implies that the energy corresponding to any wavefunction ψ which is not equivalent to the ground state wavefunction ψ_0, will always be greater than the ground state energy.[36]

Pseudopotentials

The electronic states of an atom are essentially divided into three parts - (a) *core-states* (b) *valence-states* and (c) *semi-core states*. *Core-states* refer to the innermost electronic states of the atom, which do not participate in bonding. *Valence-states* refer to the outermost electrons which participate in chemical reactions. *Semi-core states* are those states which are mostly localised and do not have a direct contribution to chemical bonding. So, in actual calculations, there is no strict necessity for precise description of the inner electrons inside the core. That brings us to pseudopotential which is an approximation for the inner orbitals to be replaced by a smooth, nodeless pseudo-wavefunction. When this potential replaces the actual potential, we have a pseudo-atomic problem, which, in essence, is not wrong but easier and faster to solve. So, pseudopotential function is used in ab initio calculations.

Bibliography

[1] http://www.undeerc.org/PCOR/Sequestration/greenhouseeffect.aspx.

[2] Pan, Y. et al. *Science* **2011**, *333*, 988–993.

[3] Foody, G. M.; Palubinskas, G.; Lucas, R. M.; Curran, P. J.; Honzak, M. *REM. SPEC. EDUC.* **1996**, *55*, 205 – 216.

[4] Canadell, J. G.; Raupach, M. R. *Science* **2008**, *320*, pp. 1456–1457.

[5] Silver, W. L.; Ostertag, R.; Lugo, A. E. *Restoration Ecol.* **2000**, *8*, 394–407.

[6] http://www.scielo.br/scielo.php?pid=S0103-90162009000200013{\&}script=sci_arttext.

[7] http://citeseerx.ist.psu.edu/viewdoc/download?doi=10.1.1.231.3339{\&}rep=rep1{\&}type=pdf.

[8] Obersteiner, M.; Azar, C.; Kauppi, P.; Mllersten, K.; Moreira, J.; Nilsson, S.; Read, P.; Riahi, K.; Schlamadinger, B.; Yamagata, Y.; Yan, J.; van Ypersele, J.-P. *Science* **2001**, *294*, 786–787.

[9] Rao, S.; Riahi, K. *Energy Journal* **2006**, *27*.

[10] Badger, P. C.; Fransham, P. *Biomass Bioenergy* **2006**, *30*, 321 – 325, Proceedings of the third annual workshop of Task 31 'Systainable production systems for bioenergy: Impacts on forest resources and utilization of wood for energy' October 2003, Flagstaff, Arizona, {USA}.

[11] Goldberg, P.; Chen, Z.-Y.; Walters, R.; Ziock, H. CO2 mineral sequestration studies. 2001.

[12] Chen, Z.-Y.; O'Connor, W. K.; Gerdemann, S. *Environ. Prog.* **2006**, *25*, 161–166.

[13] Rochelle, G. T. *Science* **2009**, *325*, pp. 1652–1654.

[14] Kheshgi, H. S. *Energy* **1995**, *20*, 915 – 922.

[15] Goldberg, D. S.; Takahashi, T.; Slagle, A. L. *Proc. Natl. Acad. Sci.* **2008**, *105*, 9920–9925.

[16] Harvey, L. D. D. *J. Geophys. Res.* **2008**, *113*, n/a–n/a.

[17] House, K. Z.; House, C. H.; Schrag, D. P.; Aziz, M. J. *Environ. Sci. Technol.* **2007**, *41*, 8464–8470.

[18] Adamczyk, K.; Prmont-Schwarz, M.; Pines, D.; Pines, E.; Nibbering, E. T. J. *Science* **2009**, *326*, 1690–1694.

[19] Gattuso, J.-P.; Frankignoulle, M.; Bourge, I.; Romaine, S.; Buddemeier, R. *Global Planet Change* **1998**, *18*, 37 – 46.

[20] Gazeau, F.; Quiblier, C.; Jansen, J. M.; Gattuso, J.-P.; Middelburg, J. J.; Heip, C. H. R. *Geophys. Res. Lett.* **2007**, *34*, n/a–n/a.

[21] Loerting, T.; Bernard, J. *ChemPhysChem* **2010**, *11*, 2305–2309.

[22] Moore, M. H.; Khanna, R.; Donn, B. *J. Geophys. Res.* **1991**, *96*, 17541–17545.

[23] Hage, W.; Hallbrucker, A.; Mayer, E. *J. Am. Chem. Soc.* **1993**, *115*, 8427–8431.

[24] Reddy, S. K.; Balasubramanian, S. *Chem. Commun.* **2014**, *50*, 503–514.

[25] Terlouw, J. K.; Lebrilla, C. B.; Schwarz, H. *Angew. Chem. Int. Ed.* **1987**, *26*, 354–355.

[26] Mori, T.; Suma, K.; Sumiyoshi, Y.; Endo, Y. *J. Chem. Phys.* **2009**, *130*, 204308.

[27] Mori, T.; Suma, K.; Sumiyoshi, Y.; Endo, Y. *J. Chem. Phys.* **2011**, *134*, 044319.

[28] Hage, W.; Liedl, K. R.; Hallbrucker, A.; Mayer, E. *Science* **1998**, *279*, pp. 1332–1335.

[29] Bernard, J.; Huber, R. G.; Liedl, K. R.; Grothe, H.; Loerting, T. *J. Am. Chem. Soc.* **2013**, *135*, 7732–7737.

[30] Bernard, J.; Seidl, M.; Kohl, I.; Liedl, K. R.; Mayer, E.; Glvez, .; Grothe, H.; Loerting, T. *Angew. Chem. Int. Ed.* **2011**, *50*, 1939–1943.

[31] Kumar, P. P.; Kalinichev, A. G.; Kirkpatrick, R. J. *J. Phys. Chem. B* **2009**, *113*, 794–802.

[32] Adamczyk, K.; Prmont-Schwarz, M.; Pines, D.; Pines, E.; Nibbering, E. T. J. *Science* **2009**, *326*, pp. 1690–1694.

[33] Moore, M.; Khanna, R. *SPECTROCHIM ACTA A* **1991**, *47*, 255 – 262.

[34] Hage, W.; Hallbrucker, A.; Mayer, E. *J. Chem. Soc., Faraday Trans.* **1996**, *92*, 3183–3195.

[35] Winkel, K.; Hage, W.; Loerting, T.; Price, S. L.; Mayer, E. *J. Am. Chem. Soc.* **2007**, *129*, 13863–13871, PMID: 17944463.

[36] `arXiv:cond-mat/0211443`.

Chapter 2

Towards the development of a force field for carbonic acid

2.1 Introduction

Carbonic acid(CA) is such a species which is present in a range of environments from the atmosphere, seawater to carbonated drinks. It is even found in our solar system as well as interstellar space.[1] It is also an important intermediate in carbon dioxide sequestration pathways where gaseous carbon dioxide is converted into mineral carbonates.[2] It has also been mentioned earlier that carbonic acid is a strong acid (pK_a = 3.45).[3] So, it is believed to play an important role in ocean acidification. Hence, it is essential to study its properties. But, the practical scenario poses a problem - it is very difficult to isolate carbonic acid. As mentioned earlier, synthesis of solid carbonic acid requires extreme and sensitive cryogenic conditions.[4] Even gas phase isolation of CA have also been done, but in inert matrix at sensitive conditions.[5] It is already known that aqueous carbonic acid, unfortunately, is very unstable and easily dissociates into bicarbonate and carbonate.[3] Hence, to facilitate the study of carbonic acid, it was proposed to develop a theoretical model of carbonic acid.

Solid carbonic acid exists in two different polymorphs - the α and the β form.[6] In the following, we have developed a theoretical model for carbonic acid and used it to elucidate the structure of one of the polymorphs of amorphous carbonic acid, namely, the β-carbonic acid.[7] Generally, the development of force field requires reproduction of some reference datawhich are mainly experimental.[8–10] In this case, the major problem associated with such an approach is finding the reference values for carbonic acid model as there are very few to almost no reference experimental values for the issue mentioned above. Hence, we adopt an approach where we calculate ab initio properties of carbonic acid using advanced quantum chemical methods like MP2[11] or M062X[12] and augmented basis sets with double, triple or quadruple zeta.[13]

Calculations have been done here for gaseous, aqueous and solid phases so as to ensure that the model reproduces the properties in all the three phases. Carbonic acid exists in three different conformers - the anti-anti, the anti-syn and the syn-syn conformer. Out of these three, the anti-anti conformer is the most stable one followed by the anti-syn conformer (the conformational difference is nearly 1.9 kcal/mol)[14] and the syn-syn conformer (the conformational energy difference is 11.8 kcal/mol)[14] respectively. So, all the calculations done here involve both anti-anti and anti-syn conformers.

The bulk phase calculations were carried out with a system of few water molecules and a carbonic acid molecule. Calculations on amorphous carbonic acid were also performed. Further description of the system used and methods used are given in the subsequent sections.

2.2 Computational Details

Calculations reported here are done using three techniques - classical, ab initio and semi-empirical.

Gas phase calculations are done to obtain information about the geometry, dipole moments and binding energies of the anti-anti (AA), anti-syn (AS) monomers and two cyclic dimers of carbonic acid. These calculations are done using Gaussian09 package[15] using second order perturbation level (MP2)[11] of theory with correlation consistent aug-cc-pVXZ[13] basis sets, where (x=D,T,Q) stands for double-ζ, triple-ζ and quadruple-ζ respectively. Carbonic acid has four different atom types. The charges of all the atom types are calculated using Merz-Singh-Kollman scheme.[16,17]

Born-Oppenheimer molecular dynamics calculations are carried out using QUICKSTEP module of CP2K software.[18] It uses a mixed basis set in which Kohn-Sham orbitals[19,20] are expanded in a Gaussian type atom-centered basis set while the electron density is represented using auxiliary plane wave basis set. Valence electrons are considered explicitly using triple-zeta molecularly optimized double-polarized basis set (TZV2P-MOLOPT-GTH).[21] The exchange-correlation functional of Becke, Lee, Yang and Parr (BLYP)[22,23] is employed. The effect of the core electrons and nuclei are accounted for by using the norm-conserving Goedecker-Teter-Hutter (GTH) pseudopotentials.[21] An energy cutoff of 280 Ry for density is used to represent the electron density. Dispersion interactions are accounted using Grimme's corrections.[24] A system consisting of 63 water molecules and one carbonic acid molecule was placed in cubic box of dimension 12.546 Å. Molecular dynamics simulations are run at 300 K with a timestep of 0.5 fs. Nosé-Hoover thermostat[25,26] is used to control the temperature of the system.

Constant pressure ensemble (NPT) simulations are carried out for the systems comprising carbonic acid molecules placed in water. TIP4P/Ice model is used to represent the interaction between water molecules.[27] Since carbonic acid force field is not available, the parameters were developed using ab initio data as a benchmark. The details of parameterization are given in next section. A time step of 0.5 fs is used to integrate equations of motion. Temperature and pressure of the

system is maintained at 300 K and 1 atm using Nosé-Hoover thermostat[25,26] and Nosé-Hoover barostat. 12-6 Lennard-Jones (LJ) functional[28] is used to calculate pairwise interactions in direct space within a cutoff distance of 8.5 Å.[27] Above this distance, long-range electrostatic interactions are calculated in reciprocal space using particle-particle particle-mesh method[29] with an accuracy of 1 part in 10^5. All water molecules are assumed to be rigid. The bonds and angles of water molecules are constrained to equilibrium values using SHAKE algorithm.[30] All 1-4 interactions are not considered during the calculations. In order to be consistent with Born-Oppenheimer calculations, a system consists of 63 water molecules and one carbonic acid molecule is taken. Initial coordinates for this run are obtained using Packmol.[31] The simulations are run for 2 ns. Since this system size is small, another system consisting 512 water molecules and one carbonic acid molecule is modelled to check for size effect. All these calculations are done using LAMMPS code.[32]

Amorphous carbonic acid is modelled using 8000 carbonic acid molecules in a cubic box whose initial coordinates were generated using Packmol software.[31] Using simulated annealing technique, four independent systems were prepared. Each of them were run for 2 ns at the temperature of 200 K.

Free energy calculations were carried out using adaptive biasing force (ABF) method.[33] These calculations were done using COLVAR package provided with LAMMPS software.[32,34] More details about this method can be found elsewhere.[35,36] A bin of size 1° was used. Free energy calculations were run for 30 ns. Biasing force was applied at every 500-th molecular dynamics step. Simulations were run for 500 ps at each value of RC and statistics were collected for every 2.5 ps. All the structures were visualised using VMD,[37] Gaussview.[38]

2.3 Results and Discussions

2.3.1 Force field development

In our approach here, we have assumed that carbonic acid has four different atom types - carbon (C, also labelled as *atom type 1*), carbonyl oxygen (O_C, also labelled as *atom type 2*), hydroxyl oxygen (O_h, also labelled as *atom type 3*) and hydrogen (H, also labelled as *atom type 4*). These are shown in Figure 2.1.

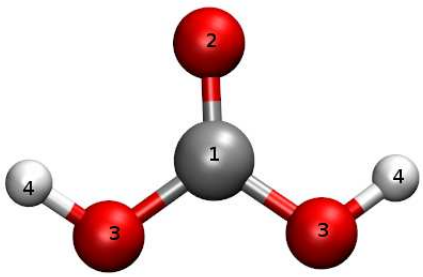

Figure 2.1: Four different atom types of carbonic acid (used here)

Cyclic dimer structures are often formed from either two monomers of anti-anti conformer or from two monomers of anti-syn conformer as shown in Figure 2.2.

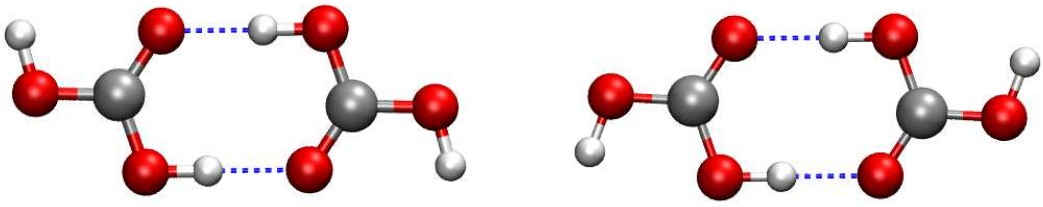

(a) anti-anti dimer **(b)** anti-syn

Figure 2.2: Carbonic acid dimers

The binding energy of such dimers is defined as

$$\Delta E = E_2 - 2(E_1) \tag{2.1}$$

where 'E_2', 'E_1' are energies of dimer and its constituent monomeric units respectively. Gas-phase binding energy of such dimers are calculated using MP2 level of theory and aug-cc-pVxZ basis sets,[13] where, x can be either D(for double-ζ) or T(for triple-ζ) or Q(for quadruple-ζ). These calculations are done in Gaussian09 package.[39]

Atomic charges of these atom types are fitted to reproduce the electrostatic potential around the anti-anti conformer (a-a) using Merz-Singh-Kollman scheme as implemented in Gaussian.[16,17,39]

Parameters

The total potential energy of a system can be written as

$$E_{total} = E_{bonded} + E_{non-bonded} \tag{2.2}$$

where E_{bonded} and $E_{non-bonded}$ are potential energies due to bonded and non-bonded interactions respectively. Further, the former term is written as a sum of four terms, as follows.

$$E_{bonded} = E_b + E_a + E_d + E_i \tag{2.3}$$

where E_b, E_a, E_d, E_i are energies due to bond stretching, angle bending, dihedral angle, and improper angle respectively. In this force field, the following analytical functional forms used to represent these terms.

Bonded Parameters The energy due to the stretching of the bonds is given by -

$$E_b = k_b(r - r_0)^2 \tag{2.4}$$

Here r describes the instantaneous bond length and r_0 describes the equilibrium bond

length. k_b describes the force constant. The initial values for the bonded parameters used in the above mentioned equation are taken from the CHARMM force field.[8] The equilibrium values are calculated from ab-initio methods. The parameters used in the above equation are given below -

Table 2.1: Bond stretching parameters

Atom	r_0 (Å)	k_b(kcal mol^{-1}(Å)$^{-2}$)
C-O_c	1.20	750.00
C-O_h	1.34	230.00
O_h-H	0.97	545.00

The contribution towards the potential energy due to the bending of the angles is given by -

$$E_a = k_a(\theta - \theta_0)^2 \tag{2.5}$$

Here θ describes the instantaneous angle and θ_0 describes the equilibrium bond length. k_b describes the force constant. The parameters used in the above equation are -

Table 2.2: Angle bending parameters

Atom	θ_0(in degree)	k_a(kcal mol^{-1}(Å)$^{-2}$)
O_c-C-O_h	125.69	50.00
O_h-C-O_h	108.61	85.00
C-O_h-H	105.7	55.00

The dihedral contribution is described by the following equation -

$$E_d = \sum_{n=1}^{5} A_n \cos^n(\delta) \tag{2.6}$$

Here δ describes the instantaneous dihedral angle. A_n represents the dihedral coefficients. The parameters are given as follows -

Table 2.3: Dihedral parameters

Atom	A_1	A_2	A_3	A_4	A_5
O_h-C-O_h-H	4.42	-0.585	-4.91	0.00	0.00
O_c-C-O_h-H	4.42	0.585	-4.91	0.00	0.00

And lastly, the improper contribution and its values are described as -

$$E_i = k_i(\phi - \phi_0)^2 \tag{2.7}$$

Table 2.4: Improper parameters

Atom	k_i(in kcal mol^{-1} radian^{-2})	ϕ_0(in degree)
C-O_c-O_h-O_h	75.00	0.00

Here ϕ represent the instantaneous value of the improper respectively; ϕ_0 describes the equilibrium value of improper respectively; k_i represent the force constants of improper.

Non-bonded parameters Non-bonded interactions are expressed as a sum of two terms - pairwise additive Lennard-Jones[28] 12-6 potential (E_{LJ}) in kcal/mol and Coulomb potential (E_{coul})[40] in kcal/mol which are expressed as,

$$E_{non-bonded} = E_{LJ} + E_{coul} \tag{2.8}$$

where

$$E_{LJ} = 4\epsilon \left[\left(\frac{\sigma}{r}\right)^{12} - \left(\frac{\sigma}{r}\right)^{6} \right] \tag{2.9}$$

$$E_{coul} = \sum_{i=1}^{N} \sum_{j=1}^{N} \frac{q_i q_j}{\epsilon r_{ij}} \tag{2.10}$$

where 'ϵ' and 'σ' are the well-depth and the distance at which the energy goes to zero respectively. 'q_i' and 'q_j' are quantities of charge on particles i and j respectively. 'ϵ' represents the dielectric constant of the medium.

The non-bonded interactions were calculated only for the atom pairs separated by four or more bonds and also for the pairs which are not bonded to each other. The 12-6 interaction coefficients between the unlike pairs of atoms were obtained using the Lorentz-Berthelot rule.[41,42] The parameters for all the non-bonded interactions are given in the table 2.5.

Table 2.5: Non-bonded parameters and charges

Atom	Type	Charge	ϵ	σ
Carbon	C	0.7000	0.0100	4.1000
Carbonyl Oxygen	O_C	-0.5920	0.1264	3.1367
Hydroxyl Oxygen	O_h	-0.5240	0.2266	2.8843
Hydrogen	H	0.4700	0.0000	0.0000

Dihedral parameterization

Potential energy surface is generated as a function of angle between planes formed by O_c-C-O_H and that of C-O_h-H at MP2/aug-cc-pVDZ level of theory.[11,13] Energies are calculated as a function of this dihedral in steps of 10°. This computed energy profile is used in the fitting procedure to obtain dihedral coefficients. Given below is a comparison between the potential energy surface obtained by using both quantum and classical calculations as a function of the above-mentioned dihedral angle.

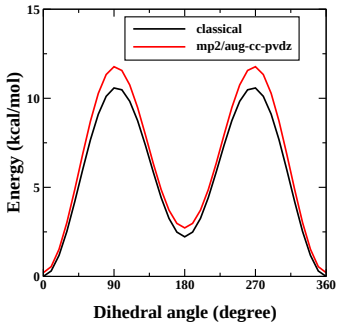

Figure 2.3: Potential Energy Surface scan with respect to change in the dihedral angle

2.3.2 Gas-phase Results

Carbonic acid monomer and dimer

Development of a robust force field involves reproduction of reference values as closely as possible. In this section, the comparison of the ab initio data and classical data for the system in gas phase is presented. The ab initio values are calculated using Density Functional Theory at the MP2 level of theory and aug-cc-pvdz basis set. These ab initio calculations have been done by Sandeep Kumar Reddy.[43]

Table 2.6: Gas phase calculation comparison

	System	Ab initio values	Force field values
Energies (kcal/mol)	Anti-Anti dimer	-22.41	-19.44
	Anti-Syn dimer	-20.27	-24.16
	Conformational difference	-1.744	-1.78
	Anti-Anti to Anti-syn Barrier	10.404	10.97
Dipole Moment(Debye)	Anti-Anti monomer	0.341	0.3505
	Anti-Syn monomer	3.951	4.3883

These calculations were done at zero kelvin temperature using the Gaussian G09 package.[39] From these calculations, it is observed that this force field reasonably agrees with the gas phase data.

Potential Energy Surface Scans

Potential Energy Surface Scans refer to the exploration of potential energy surface as a function of one or more degrees of freedom.[15] Such degrees of freedom can be either change in bond length or rotation of bond angle or rotation in dihedral angle and so on. There can be two types of potential energy surface scans -

1. **Rigid Potential Energy Surface Scans**

Here, for every value of the reaction coordinate, the single point energy of the system is calculated. The internal geometry and other degrees of freedom are assumed to be rigid and unchanged.

2. **Relaxed Potential Energy Surface Scans**

For every value of reaction coordinate, a geometry optimisation of the system is done. Thus, the different degrees of freedom of the system is allowed to relax and hence the name.

Here we have done some rigid potential energy surface scans between carbonic acid and water. Depending on the position of the minimum of the curve, we have an idea about the equilibrium distance between the two species. Also, information on the energy of the equilibrated system can be obtained from the same. These also tell us about the most feasible orientation of interaction between the two species. Three different orientations of carbonic acid and water were taken for such calculations.

The results for the anti-anti monomer are given in the following figures.

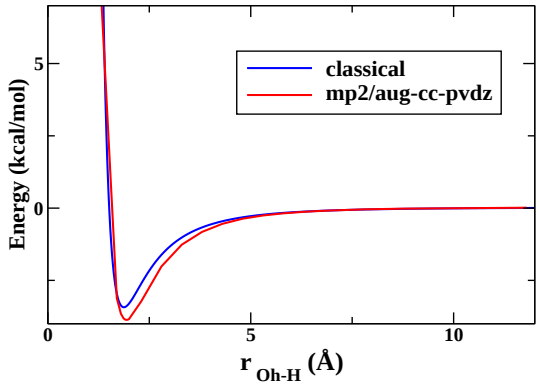

(a) scan along $O_{hydroxyl}$-H_{water}

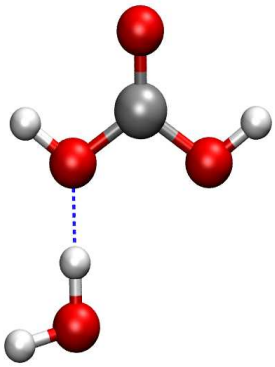

(b) $O_{hydroxyl}$-H_{water}

Figure 2.5: Gas phase scan along $O_{hydroxyl}$ - H_{water} interaction for Anti-Anti conformer of carbonic acid

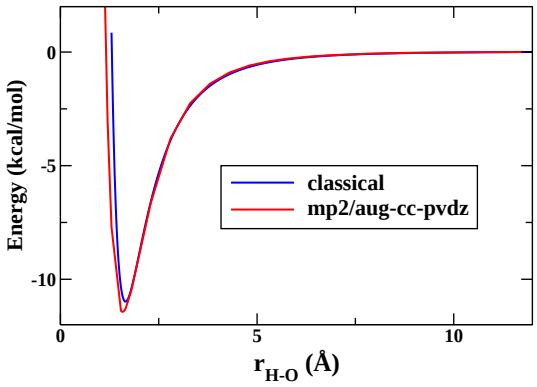

(a) scan along $H_{carbonic}$-O_{water}

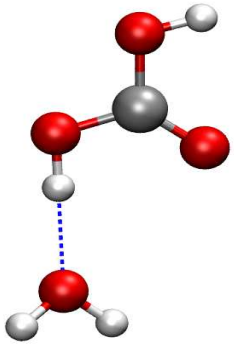

(b) $H_{carbonic}$-O_{water}

Figure 2.6: Gas phase scan along $H_{carbonyl}$ - O_{water} interaction for Anti-Anti conformer of carbonic acid

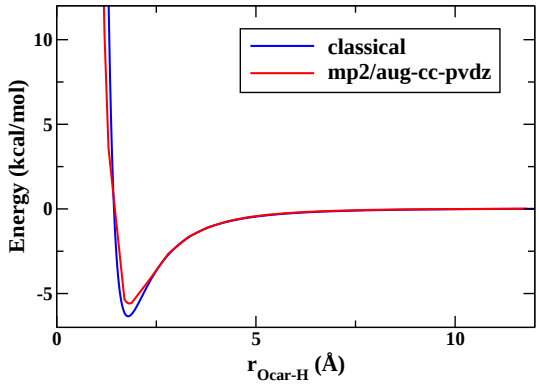

(a) scan along $O_{carbonyl}$-H_{water}

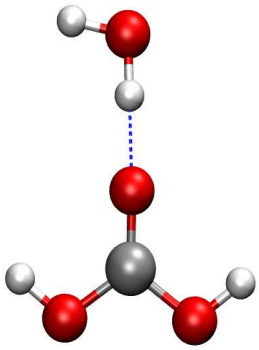

(b) $O_{carbonyl}$-H_{water}

Figure 2.4: Gas phase scan along $O_{carbonyl}$ - H_{water} interaction for Anti-Anti conformer of carbonic acid

The results for the anti-syn conformer are given in the following figures.

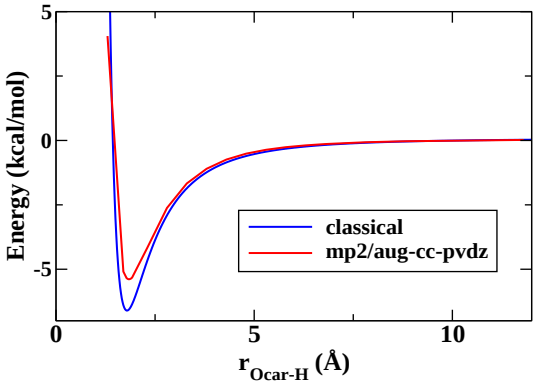

(a) scan along $O_{carbonyl}$-H_{water}

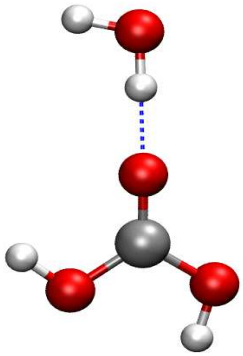

(b) $O_{carbonyl}$-H_{water}

Figure 2.7: Gas phase scan along $O_{carbonyl}$ - H_{water} interaction for Anti-Syn conformer of carbonic acid

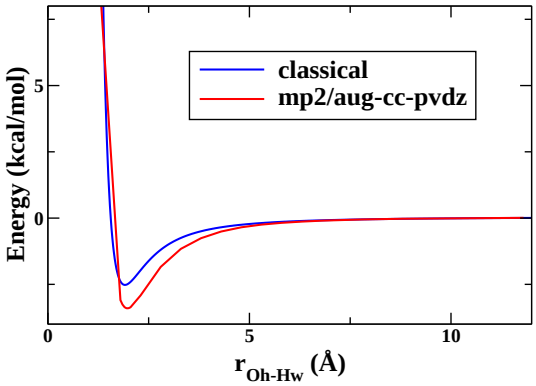

(a) scan along $O_{hydroxyl}$-H_{water}

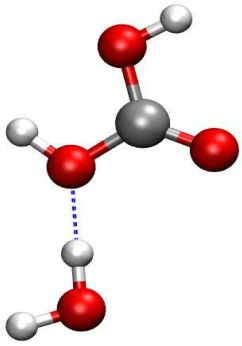

(b) $O_{hydroxyl}$-H_{water}

Figure 2.8: Gas phase scan along $O_{hydroxyl}$ - H_{water} interaction for Anti-Syn conformer of carbonic acid

In all the above cases, the blue curve represents the results from classical calculation or force-field calculation and the red curve represents the results from ab initio calculation. We scale the ab initio curves by a factor of 1.4256, which is obtained from the ratio of binding energy of water dimer as given by ab initio methods to that given by tip4p/ice water model.[27] Such kind of scaling is not uncommon and have been earlier done in the development of many other force fields.[44] It is seen that for both the conformers, the force-field seems to reproduce the ab initio data

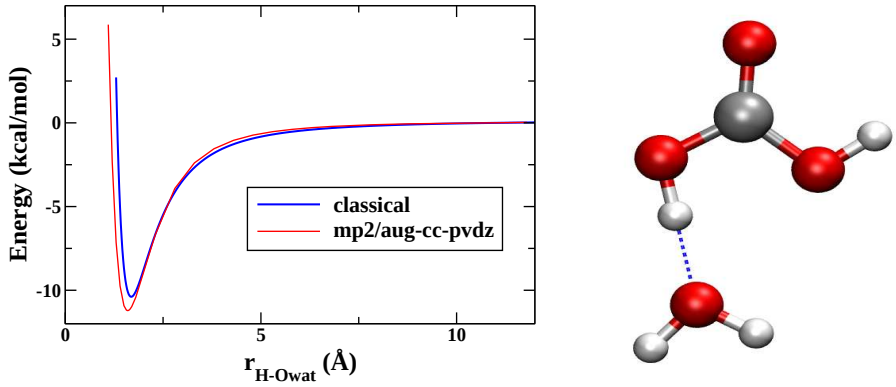

(a) scan along $H_{carbonic}$-O_{water} **(b)** $H_{carbonic}$-O_{water}

Figure 2.9: Gas phase scan along $H_{carbonic}$ - O_{water} interaction for Anti-Syn conformer of carbonic acid

quite closely.

2.3.3 Bulk phase results

NPT and NVT molecular dynamics simulations were carried out at 300K temperature and atmospheric pressure on a system consisting of 63 water molecules and 1 carbonic acid. Timestep of 1 femtosecond was used in the calculations and Velocity Verlet algorithm was used for the force calculation. Then, it was equilibrated for 2 ns before further calculation. This was done for both the monomers - the anti-anti(AA) and the anti-syn(AS) monomer.

Pair correlation function

Pair correlation functions (pcf), represented as g(r), gives the probability of finding one particle at a given distance, r, from the center of another particle. It is the ratio of actual distribution of molecules around a given particle to the ideal distribution around it. Thus, at shorter distances, it sheds light on how the particles are packed together. Hence, actual distribution at shorter distance is more. So, g(r) is much greater than 1 at shorter distances. But, at longer distances, the coordination layers become more diffuse and the ratio of actual to real distributuion becomes equal to

one. Hence g(r) normalises to 1 at larger distances.[45]

The position and the amplitude of the first and most prominent peak gives information about the environment of the system. Here, we calculated the pair correlation functions between all the different atom types of carbonic acid and water molecules. These pair correlation functions were calculated with a bin width of 0.1 Å. We have calculated pair correlation functions both for a system containing 63 water molecules and 1 carbonic acid as well as for a system containing 512 water molecules and 1 carbonic acid. This was done to test the effect of increase in system size on the Pair correlation functions. All of this is represented in the figures 2.10 and 2.11, first for the AA monomer and water, then for the AS monomer and water.

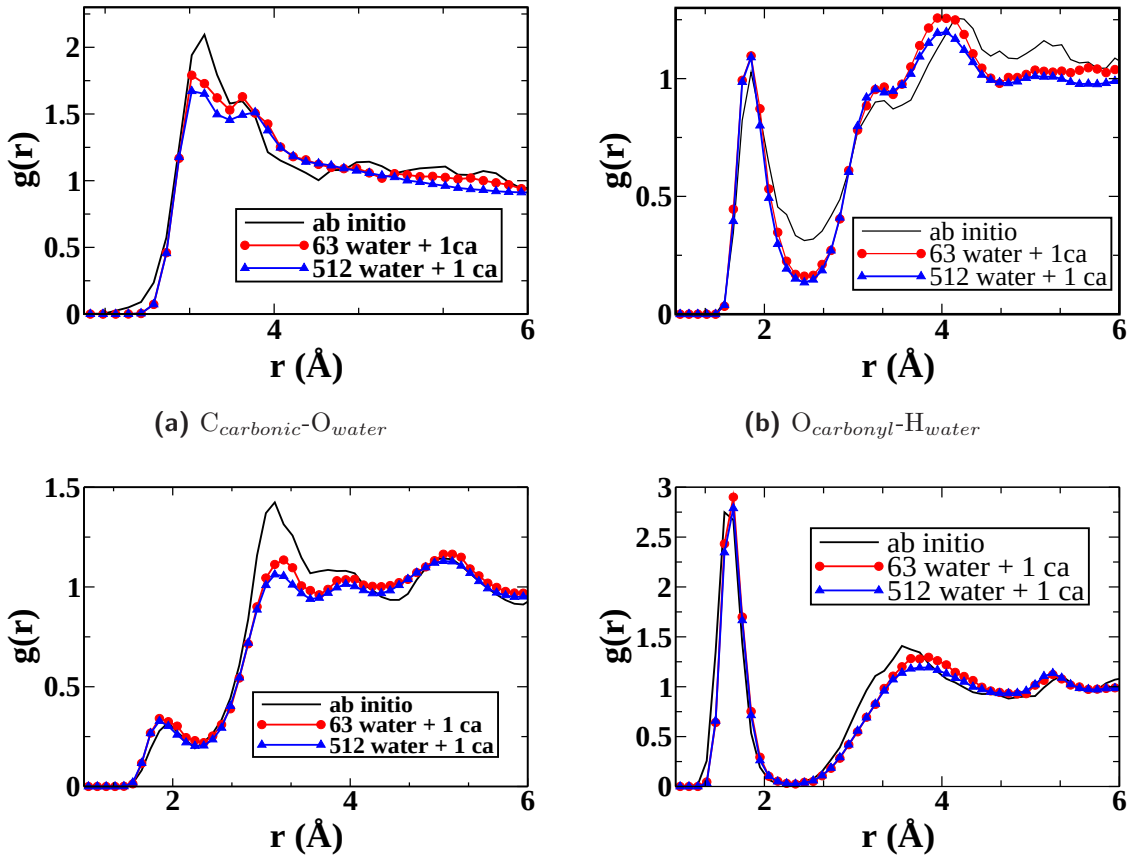

(a) $C_{carbonic}$-O_{water} **(b)** $O_{carbonyl}$-H_{water}

(c) $O_{hydroxyl}$-H_{water} **(d)** $H_{carbonic}$-O_{water}

Figure 2.10: Comparison of pair correlation functions between different atom types of anti-anti monomer of carbonic acid for two systems of 63 water molecules and 1 carbonic acid and 512 water molecules and 1 carbonic acid

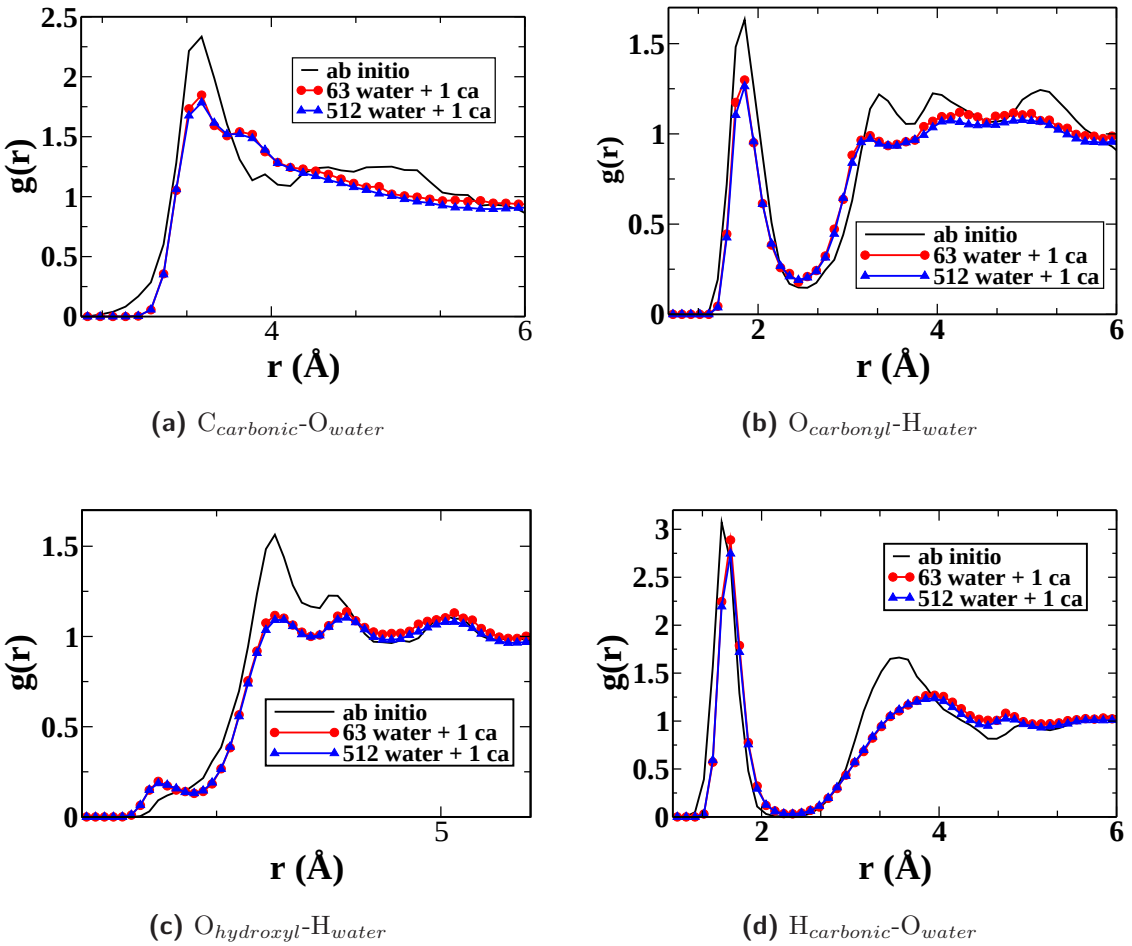

(a) $C_{carbonic}$-O_{water} **(b)** $O_{carbonyl}$-H_{water}

(c) $O_{hydroxyl}$-H_{water} **(d)** $H_{carbonic}$-O_{water}

Figure 2.11: Comparison of pair correlation functions between different atom types of anti-syn monomer of carbonic acid for two systems of 63 water molecules and 1 carbonic acid and 512 water molecules and 1 carbonic acid

Since pcf gives an idea about the short-range structure of the system, we expected that the change in system size will not affect the pair correlation functions between different atom types. The immediate environment would still be the same. These figures confirm our anticipation that the increase in size of the system does not affect the pair correlation functions between the different atom types. From the bulk phase calculations also, it can be concluded that the developed force field seems to reproduce the ab initio data really well.

2.3.4 Amorphous Carbonic Acid

It is already known that carbonic acid exists in two polymorphic forms - the α and β forms, depending on whether methanolic solution or aqueous solution was used during its synthesis.[46,47] Some earlier vibrational studies have been done to investigate the structure of β-carbonic acid.[48] But, the crystal structure of the amorphous β-carbonic acid has not been elucidated yet. But, from powder X-ray data, we came to know that the β-carbonic acid has a broad feature at 27°.[49] Our purpose was to explore the structure of amorphous β-carbonic acid by the help of the model we developed.

We approached the problem by starting with four different initial configurations of amorphous carbonic acid. Each system consisted of 8000 molecules of carbonic acid. These configurations were obtained by heating the same system randomly to different temperatures followed by cooling to 200K and equilibration for at least 2 ns. During such simulations, atmospheric pressure was maintained. The final box length of such a system was approximately 164 Å. MD simulations were carried out on these systems using the newly developed force field parameters.

Structure Factor and X-Ray Powder Diffraction Pattern

In crystallography, structure factor provides information on how the X-rays are scattered by a material. The intensity of this scattered X-ray gives an idea about the structure of the material. It is calculated as a function of wave vector, q which is calculated by the Fourier Transform of distance as[50] -

$$F(k) = \int_{-\infty}^{\infty} f(x) e^{-i2\pi kx} dx \tag{2.11}$$

The partial structure factor, in turn, is calculated using the following formula from the wave vector, q, as[51] -

$$S_{\alpha\beta}(q) = \delta_{\alpha\beta} + 4\pi\sqrt{\rho_\alpha \rho_\beta}\int_0^\infty r^2[g_{\alpha\beta}(r) - 1]\frac{sin(qr)}{(qr)}dr \tag{2.12}$$

where $\delta_{\alpha\beta}$ represents the Kronecker delta, ρ_α and ρ_β represent the number density of species α and β respectively in the system. From these, the total structure factor is calculated using the following formula,

$$S(q) = \sum_\alpha \sum_\beta c_\alpha c_\beta \frac{f_\alpha(q) f_\beta(q)}{\left\langle f(q)\right\rangle^2} S_{\alpha\beta}(q) \tag{2.13}$$

where c_α and f_α are concentration and scattering length (or form factor) of atom type α in the system respectively. where, $\left\langle f(q)\right\rangle = \sum_\alpha c_\alpha f_\alpha(q)$.
The X-ray scattering intensity is calculated as the square of the total structure factor. This intensity is plotted as a function of 2θ. Cu-Kα X-ray(wavelength 1.54 Å) is used. This powder pattern appears as -

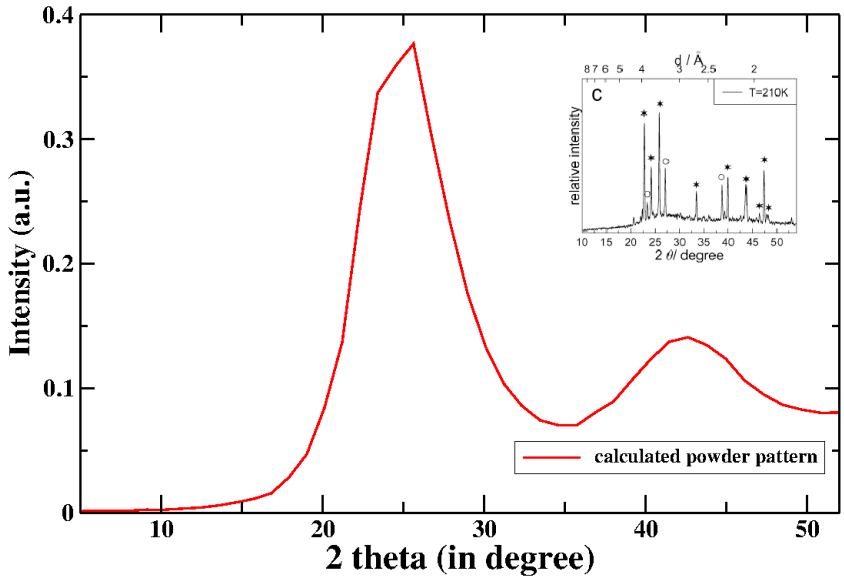

Figure 2.12: X-ray Powder patterns (Cu-Kα rays of wavelength λ=1.54Å) of amorphous carbonic acid obtained from classical calculations. Inset: Experimental powder pattern.[49] The broad feature centered at 27° corresponds to amorphous β-carbonic acid.

From our calculation, the peak with the maximum intensity appears at 24°. In order to understand the atom types which actually contribute to that peak, we looked into

the partial structure factors and weighted partial structure factors of all the different types of atom pairs. Here, weighted partial structure factors are nothing but the product of the concentration and the form factors of the corresponding pairs in the system. They appear as -

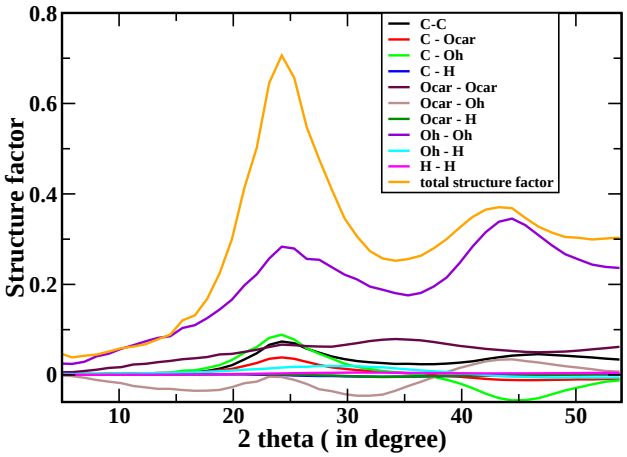

Figure 2.13: Comparison of pairwise weighted partial structure factors for all the pairs and the total structure factor

The immediate conclusion drawn from this figure is that the maximum contribution comes from the pair type interaction between O_h-O_h. Both curves show a peak at around 24.5 °. But, the powder pattern of amorphous α and β carbonic acid has already been reported by Loerting et al in 2007.[49] They reported a prominent peak at 27° for β-carbonic acid.

2.3.5 Free energy calculation

Energy difference between AA and AS conformers is 1.74 kcal/mol in gas phase. In water, due to difference in hydrogen bonding between water molecules and each of these conformers, one of them may get more stabilized than the other. In order to understand the influence of water molecules, free energy calculations are carried out at the temperature 300 K using adaptive biasing force method. Two types of

reactions coordinates can be used to study conformational energy difference - dihedral angle (O_C-C-O_H-H) and coordination number. In this case, the coordination number is defined as the number of H atoms of carbonic acid around the O_H atoms. Since the harmonic function, which is used for bond stretching do not allow for the proton dissociation, the latter reaction coordinate cannot be used. Hence, we used the dihedral angle (O_C-C-O_H-H) as reaction coordinate.

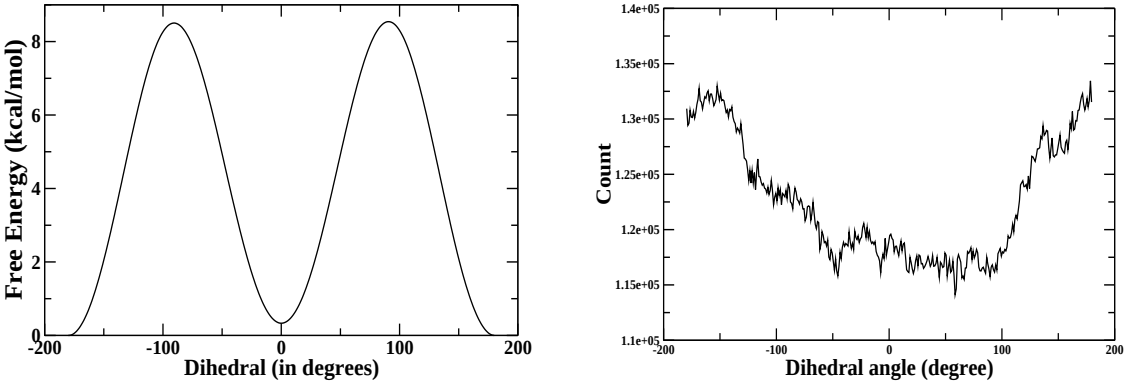

Figure 2.14: Left panel: Free energy difference between anti-anti and anti-syn conformers. The dihedral angle values of 0° and 180° correspond to anti-anti and anti-syn conformers respectively. Right panel: Histogram as a function of dihedral.

Figure 2.14 (left panel) shows the free energy calculated as a function of dihedral. It shows that anti-anti conformer is less stable than anti-syn conformer, contrary to gas-phase calculations. The energy difference between two conformers is 0.31 kcal/mol whereas the gas phase value is 1.74 kcal/mol (at MP2 level of theory and aug-cc-pVdz basis set). These values suggest that the anti-anti conformer is less stabilized in water than anti-syn conformer. The values reported here are different compared to the values reported by Galib and Hanna, in 2011.[52] They reported the energy difference as 2.5 kcal/mol. This difference in free energy values might be due to different free energy methods. However, their calculations support the stability of anti-anti conformer over anti-syn conformer in the aqueous phase. But some earlier studies[53] found similar results. They explained it on the basis of the differential

strength of the hydrogen bond formed in aqueous solution by two different conformers. The convergence of free energy calculations is also checked by calculating the ratio of N_1/N_2 where 'N_1' and N_2 are maximum and minimum values in the histogram as shown in Figure 2.14 (right panel). In this case, the ratio is close to '1' which suggests the convergence of free energy. During conformer change, a high potential is imposed on the neighbouring water coordination shells than compared to the case where the coordination number is used as a reaction coordinate. To know the exact free energy barrier, one has to use other reaction coordinate (coordination number) which is not possible with force field. One can guess at this point that the free energy barrier will be definitely less than 10.34 kcal/mol.

2.4 Conclusions

We have tried to model such a compound which is crucial in numerous aspects of nature but has almost negligible experimental data. As a result, we do not have traditional reference values for carbonic acid. So, here, in this work instead of benchmarking ab initio calculations against experimental values, we use ab initio values as our benchmark.

The development involves checking the reproduction of ab initio values in all the three phases - the gas phase, the aqueous phase and the solid amorphous phase. There are only four different atom types defined here- the carbon, the carbonyl oxygen, the hydroxyl oxygen and the hydrogen. Charges on them are calculated using Merz-Kollmann scheme.

In the gas phase, the binding energy of the dimers of carbonic acid are calculated along with the dipole moment values of the carbonic acid monomer at 0 K and atmospheric pressure. Such comparison serves as a test whether the force field can reproduce gas phase isolated molecular features. From Table 2.6, we saw that the force-field can reproduce such gas-phase data appreciably. Apart from this, rigid

potential energy surface scans were also done to test if the force-field was able to reproduce the behaviour of the system when one carbonic acid interacted with one water molecule in the gas phase for all possible orientations. Even, in this case too, it showed a likewise behaviour.

Coming to a little more complicated system like bulk water and carbonic acid at room temperature and atmospheric pressure, we carried out both ab initio and classical MD simulations. Properties calculated from both MD simulations, like g(r), also showed similar trend, when compared. Thus, this model could reproduce the bulk phase properties too.

And finally, for amorphous state, we calculated the X-ray powder pattern and found that the peak of the maximum intensity is at 24° whereas from experiments, this peak appears at 27°. Thus, this model, even though is able to reproduce the gas phase and bulk phase values, does not produce such a good match for amorphous state (a difference of 3°). However, we have, for the first time, developed a theoretical model for carbonic acid which may not be that robust, but is able to express many properties quite well.

Finally the free energy calculations also support the trend that the *anti-anti* conformer is the most stable one out of the three. The challenge now, is to use this force field so as to get a better insight into the chemistry of carbonic acid and take a step closer towards carbon dioxide sequestration.

Bibliography

[1] Hage, W.; Liedl, K. R.; Hallbrucker, A.; Mayer, E. *Science* **1998**, *279*, pp. 1332–1335.

[2] Reddy, S. K.; Balasubramanian, S. *Chem. Commun.* **2014**, *50*, 503–514.

[3] Loerting, T.; Bernard, J. *ChemPhysChem* **2010**, *11*, 2305–2309.

[4] Moore, M. H.; Khanna, R.; Donn, B. *J. Geophys. Res. Planets* **1991**, *96*, 17541–17545.

[5] Mori, T.; Suma, K.; Sumiyoshi, Y.; Endo, Y. *J. Chem. Phys.* **2009**, *130*, 204308.

[6] Hage, W.; Hallbrucker, A.; Mayer, E. *J. Chem. Soc., Faraday Trans.* **1996**, *92*, 3183–3195.

[7] Reddy, S. K.; Kulkarni, C. H.; Balasubramanian, S. *J. Chem. Phys.* **2011**, *134*, 124511.

[8] Brooks, B. R. et al. *J. Comp. Chem.* **2009**, *30*, 1545–1614.

[9] Huang, L.; Roux, B. *J. Chem. Theo. Comp.* **2013**, *9*, 3543–3556.

[10] Nielson, K. D.; van Duin, A. C. T.; Oxgaard, J.; Deng, W.-Q.; Goddard, W. A. *J. Phys. Chem. A* **2005**, *109*, 493–499.

[11] Head-Gordon, M.; Pople, J. A.; Frisch, M. J. *Chem. Phys. Lett.* **1988**, *153*, 503 – 506.

[12] Zhao, Y.; Truhlar, D. *Theo. Chem. Acc.* **2008**, *120*, 215–241.

[13] Dunning, T. H. *J. Chem. Phys.* **1989**, *90*, 1007–1023.

[14] Wight, C. A.; Boldyrev, A. I. *J. Phys. Chem.* **1995**, *99*, 12125–12130.

[15] Frisch, M. J. et al. Gaussian 09. Gaussian Inc. Wallingford CT 2009.

[16] Singh, U. C.; Kollman, P. A. *J. Comp. Chem.* **1984**, *5*, 129–145.

[17] Besler, B. H.; Merz, K. M.; Kollman, P. A. *J. Comp. Chem.* **1990**, *11*, 431–439.

[18] VandeVondele, J.; Krack, M.; Mohamed, F.; Parrinello, M.; Chassaing, T.; Hutter, J. *Comput. Phys. Commun.* **2005**, *167*, 103 – 128.

[19] Hohenberg, P.; Kohn, W. *Phys. Rev.* **1964**, *136*, B864–B871.

[20] Kohn, W.; Sham, L. J. *Phys. Rev.* **1965**, *140*, A1133–A1138.

[21] Goedecker, S.; Teter, M.; Hutter, J. *Phys. Rev. B* **1996**, *54*, 1703–1710.

[22] Lee, C.; Yang, W.; Parr, R. G. *Phys. Rev. B* **1988**, *37*, 785–789.

[23] Becke, A. D. *Phys. Rev. A* **1988**, *38*, 3098–3100.

[24] Grimme, S. *J. Comp. Chem.* **2006**, *27*, 1787–1799.

[25] Nosé, S. *J. Chem. Phys.* **1984**, *81*, 511–519.

[26] Hoover, W. G. *Phys. Rev. A* **1985**, *31*, 1695–1697.

[27] Abascal, J. L. F.; Sanz, E.; Garcia Fernndez, R.; Vega, C. *J. Chem. Phys.* **2005**, *122*, 234511.

[28] Jones, J. E. *Proceedings of the Royal Society of London. Series A* **1924**, *106*, 463–477.

[29] Hockney,; Eastwood, *Computer Simulation Using Particles*; Taylor and Francis: 270, Madison Avenue, New York, 10016, 1988.

[30] Forester, T. R.; Smith, W. *J. Comp. Chem.* **1998**, *19*, 102–111.

[31] Mart´inez, L.; Andrade, R.; Birgin, E. G.; Mart´inez, J. M. *J. Comput. Chem.* **2009**, *30*, 2157–2164.

[32] Plimpton, S. *J. Comp. Phys.* **1995**, *117*, 1 – 19.

[33] Darve, E.; Pohorille, A. *J. Chem. Phys.* **2001**, *115*, 9169–9183.

[34] Fiorin, G.; Klein, M. L.; Hnin, J. *Mol. Phys.* **2013**, *111*, 3345–3362.

[35] Rodriguez-Gomez, D.; Darve, E.; Pohorille, A. *J. Chem. Phys.* **2004**, *120*, 3563–3578.

[36] Darve, E.; Rodrguez-Gmez, D.; Pohorille, A. *J. Chem. Phys.* **2008**, *128*, 144120.

[37] Humphrey, W.; Dalke, A.; Schulten, K. *J. Mol. Graphics* **1996**, *14*, 33–38.

[38] Dennington, R.; Keith, T.; Millam, J. GaussView Version 5. Semichem Inc. Shawnee Mission KS 2009.

[39] Frisch, M. J. et al. Gaussian 09 Revision D.01. Gaussian Inc. Wallingford CT 2009.

[40] de Coulomb, C.-A. Premier mmoire sur llectricit et le magntisme. Histoire de l'Academie royale des sciences.

[41] Lorentz, H. A. *Annalen der Physik* **1881**, *248*, 127–136.

[42] Berthelot, D. *Comptes rendus hebdomadaires des sances de l'Acadmie des sciences* **1898**, *126*, 1703–1855.

[43] Dr. Sandeep Kumar Reddy, {`https://sites.google.com/site/kumar0020/`}.

[44] MacKerell, A. D. et al. *J. Phys. Chem. B* **1998**, *102*, 3586–3616.

[45] `http://www.physics.emory.edu/faculty/weeks//idl/gofr.html`.

[46] Hage, W.; Hallbrucker, A.; Mayer, E. *J. Chem. Soc., Faraday Trans.* **1995**, *91*, 2823–2826.

[47] Hage, W.; Hallbrucker, A.; Mayer, E. *J. Am. Chem. Soc.* **1993**, *115*, 8427–8431.

[48] Reddy, S. K.; Kulkarni, C. H.; Balasubramanian, S. *J. Phys. Chem. A* **2012**, *116*, 1638–1647.

[49] Winkel, K.; Hage, W.; Loerting, T.; Price, S. L.; Mayer, E. *J. Am. Chem. Soc.* **2007**, *129*, 13863–13871.

[50] `http://topex.ucsd.edu/geodynamics/01fourier.pdf`.

[51] Raju, S. G.; Balasubramanian, S. *J. Phys. Chem. B* **2009**, *113*, 4799–4806.

[52] Galib, M.; Hanna, G. *J. Phys. Chem. B* **2011**, *115*, 15024–15035.

[53] Tossell, J. *Geochimica et Cosmochimica Acta* **2005**, *69*, 5647 – 5658.

Chapter 3

Quantum Chemical Investigations of Carbon dioxide-Lewis base complexes

3.1 Introduction

In 1923, G.N. Lewis first introduced the concept of Lewis acids and bases.[1] He proposed that Lewis acids are electron acceptors whereas Lewis bases are electron donors. From this, it directly follows that species with one or more lone pairs or negative charges, i.e., with higher electron density, like amines, oxides or anionic species behave as Lewis bases. Species with lower electron density, like BF_3 or positively charged species behave as Lewis acids.

The nature of interaction between a Lewis base and a Lewis acid is not necessarily electrostatic. It rather involves the transfer of electron density from one Highest Occupied Molecular Orbital (HOMO) of the Lewis Base to the Lowest Unoccupied Molecular Orbital (LUMO) of the Lewis acid. This, in turn leads to the formation of an electron donor-acceptor complex between the acid and the base. Thus,

Lewis bases have a highly localised HOMO. Lewis acids have highly localised, empty atomic or molecular orbital of lower energy (LUMO). Such a LUMO can accomodate a pair of electrons.[2] There is no direct measurement of the Lewis acid-base strength; however, the strength of the interaction between the acid and base in the adduct formed gives a rough estimate of the same.[3]

Carbon dioxide is a well known and abundant molecule. It can also act as a Lewis acid. It has no dipole moment. The carbon, here, is not only sp hybridised, but is also flanked on both sides by two electronegative oxygen atoms. These factors render the carbon center highly electron deficient in nature. So, it acts as a Lewis acid in presence of Lewis bases like amine and other negatively charged species. Evidences from infra-red spectroscopy[4] and ab-initio calculations[5] are also suggestive of such behaviour of CO_2.

This particular property of carbon dioxide is exploited in a wide variety of fields. As mentioned earlier, in section 2.3.1 of Chapter 1, one of the methods involved in carbon dioxide sequestration is the use of chemical scrubbers. Generally, compounds used as scrubbers contain electron-rich groups like amines[6] which act as Lewis bases and interact with the Lewis acidic CO_2 thus removing it from any gas stream.

Another different group of chemical compounds, namely amidophosphoranes containing four-membered rings, are also used to capture atmospheric gaseous carbon dioxide.[7] The phosphorus atom containing electron lone pairs act as electron donor and interacts with CO_2.

Similar to scrubbers, use of Metal-Organic Frameworks (MOFs) to capture atmospheric gaseous CO_2 are also common. These MOFs generally have a Lewis basic center which interacts with the CO_2. For example, in a MOF made of $Fe_3(CO_2)_6$ sulphate clusters (the metal part) and linear chains of phenyl or biphenyl groups

(the organic linker), there is an interaction between the Lewis basic carbonyl oxygen(present in the metal part) and Lewis acidic carbon dioxide which results in capturing atmospheric carbon dioxide.[8]

Ionic liquids are also another class of compounds which are made up of ion pairs. These are also used for carbon dioxide capture due to such similar type of interactions, that is, Lewis acid and base interactions.[9]

Supercritical CO_2 is used in the synthesis of polymer poly(1,1-dihydroperfluorooctyl acrylate). The Lewis acid-base interactions between CO_2 and the acrylate group is believed to stabilise the polymer.[10] The solubility of certain nonvolatile compounds in supercritical carbon dioxide-cosolvent mixtures also increases due to this acid-base interaction.

Thus, keeping in mind the importance of such Lewis acid-base interactions, we have studied the interaction between 27 Lewis bases (nitrogen and oxygen being donor atoms in most cases) and the Lewis acid, carbon dioxide, CO_2. We have compared their strength of interaction through binding energy calculations using ab initio methods.

3.2 Computational Details

Ab initio calculations have been done on (a) only CO_2 (b) only bases (c) base and CO_2 . The density functional method M062X is used for these calculations.[11] The basis set used here is 6-31+g(d,p).[12–14]

Only gas-phase calculations are reported here. The calculations have been done at 0K. A set of 26 bases have been used for the calculations.[3] These are acetone,

aniline, acetonitrile, diethylamine, diisopropylamine, dimethylethylamine, di-tert-amylamine, dimethylformamide, dimethylsulfoxide, ethanol, ethylmethylamine, isopropylamine, isoquinoline, n-butylamine, piperidine, propylamine, pyridine, pyrrolidine, quinoline, quinuclidine, tert-amylamine, tetra-hydrofuran, triethylamine, triisopropylamine, tropane and tris-2-ethylhexylamine.

At first, one isolated CO_2 molecule and one isolated molecule of each of the bases are optimised separately. The optimised structures of the isolated base and the CO_2 are taken together to calculate the interaction between them. Initially, optimisations involving base and CO_2 are done in almost three to four orientations for each of the bases. Depending on the possibility of the Lewis acid to approach the Lewis base, calculations are done along these orientations. This approach helps to explore the potential energy surface better.

Once we compare the energy of all the different optimised Lewis base - CO_2 complex, we have an estimate of the lowest energy structure out of all these for each of the different bases. This lowest energy Lewis base-CO_2 arrangement is taken for further calculation to remove the basis set superposition error (BSSE).[15] The optimised geometry and the corresponding energy values are reported here.

The binding energy of the Lewis base and CO_2 adduct is calculated in the following manner -

$$Binding\ Energy_{(LB+CO_2)} = E_{LB+CO_2} - (E_{LB} + E_{CO_2}) \tag{3.1}$$

where LB denotes Lewis base, E_{LB+CO2} denotes the energy of the Lewis base and CO_2 adduct, E_{LB} denotes the energy of the isolated Lewis base and E_{CO2} denotes the energy of the isolated carbon dioxide molecule. The values reported here are for the lowest energy arrangement, both with and without BSSE correction. They are shown in Table 1 along with the O-C-O bond angle of CO_2. These calculations have been done using the gaussian09 package.[16] The visualisation software used is

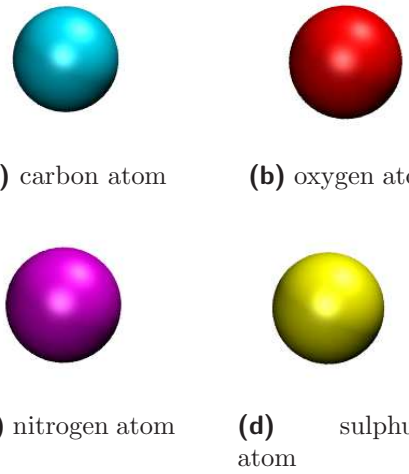

(a) carbon atom **(b)** oxygen atom

(c) nitrogen atom **(d)** sulphur atom

Figure 3.1: Colour codes for different atom types

gaussview.[17]

3.3 Results and Discussion

3.3.1 Geometry

Figure 1 shows the colour code used in the figures for the different atom types. The geometry optimised structures of the Lewis Base - CO_2 complex for all the 26 bases are shown here.All these structures correspond to the lowest energy arrangement, as mentioned in the earlier section.

The binding energy of all these CO_2 - base adducts are given in the table 3.1. Both bsse corrected and without bsse correction are reported here. Also, the O-C-O bond angle is given here for all the adducts. There are different trends observed for bases of different structures.

3.3.2 Analysis

For the acyclic amines, in general, the relative order of binding strength of the base-CO_2 complex increases in the order of primary amine < secondary amine < tertiary

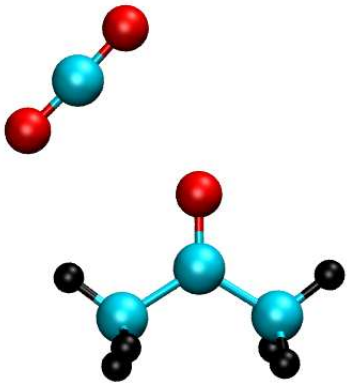

(a) acetone-CO_2 adduct

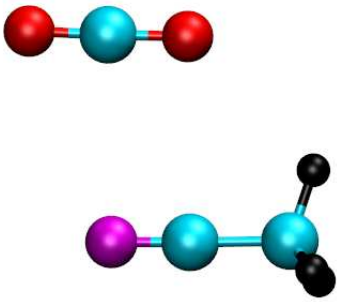

(b) acetonitrile-CO_2 adduct

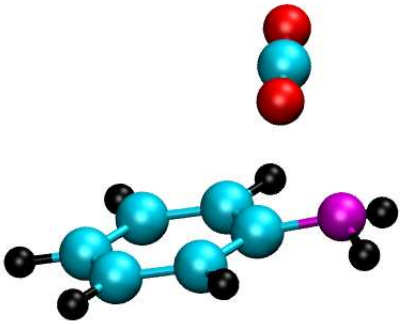

(c) aniline-CO_2 adduct

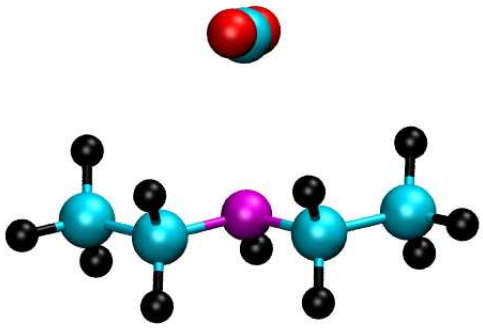

(d) diethylamine-CO_2 adduct

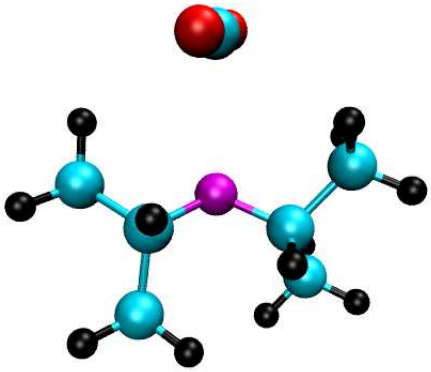

(e) diisopropylamine-CO_2 adduct

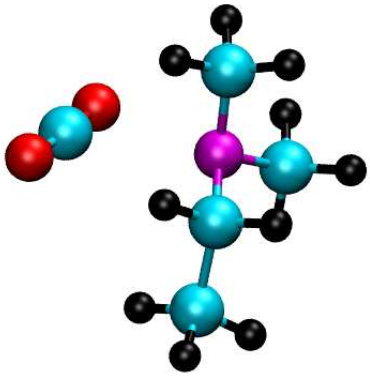

(f) dimethylethylamine-CO_2 adduct

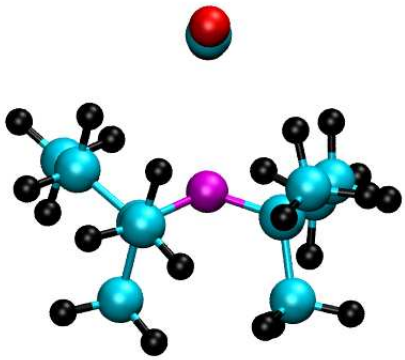

(a) di-tert-amylamine-CO_2 adduct

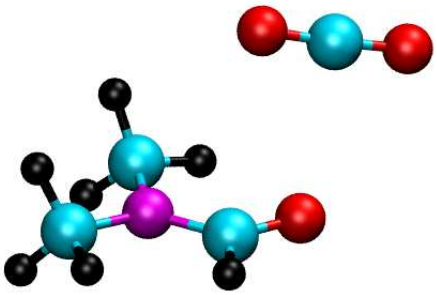

(b) dimethylformamide-CO_2 adduct

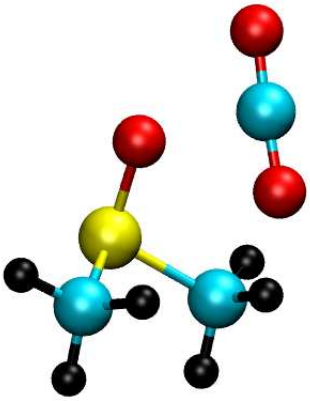

(c) dimethylsulfoxide-CO_2 adduct

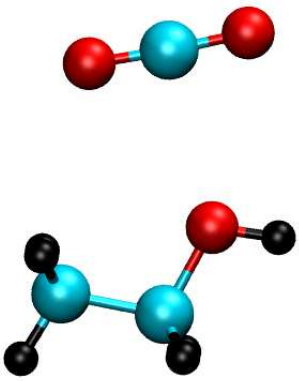

(d) ethanol-CO_2 adduct

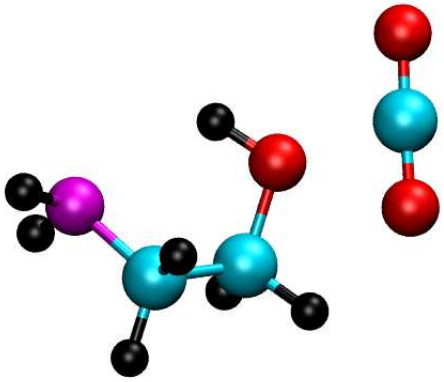

(e) ethanolamine-CO_2 adduct

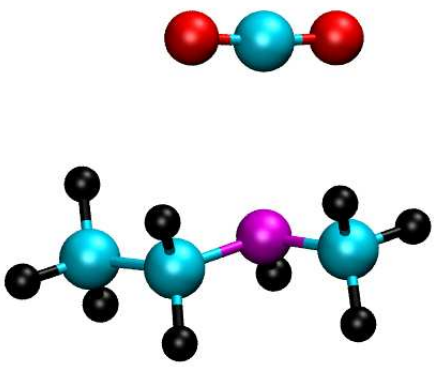

(f) ethylmethylamine-CO_2 adduct

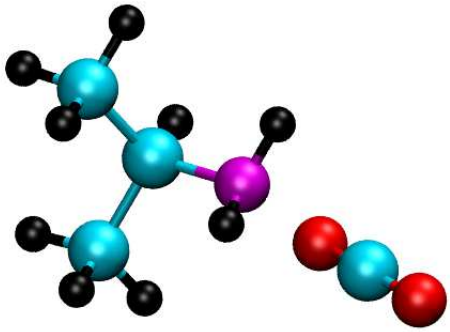

(a) isopropylamine-CO_2 adduct

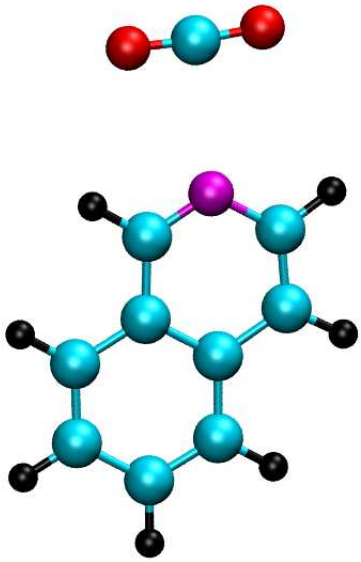

(b) isoquinoline-CO_2 adduct

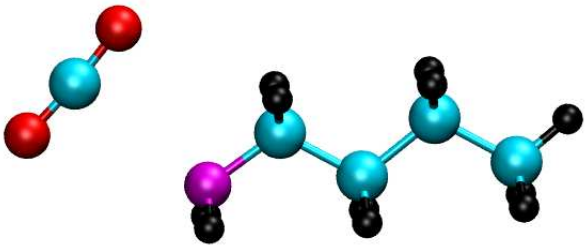

(c) n-butylamine-CO_2 adduct

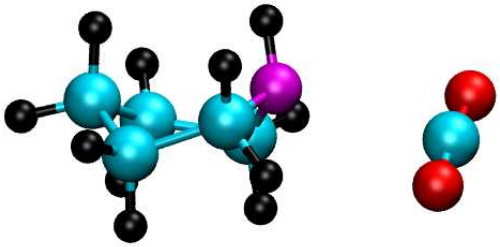

(d) piperidine-CO_2 adduct

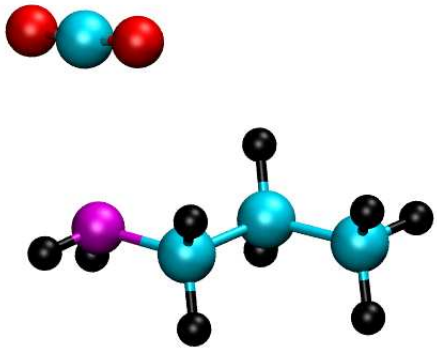

(e) propylamine-CO_2 adduct

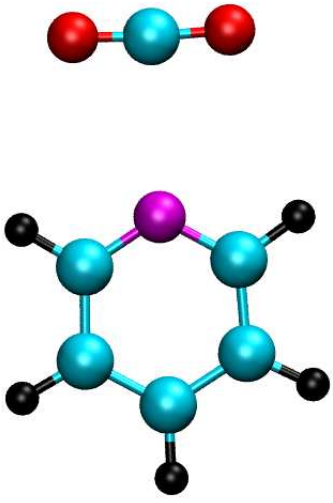

(f) pyridine-CO_2 adduct

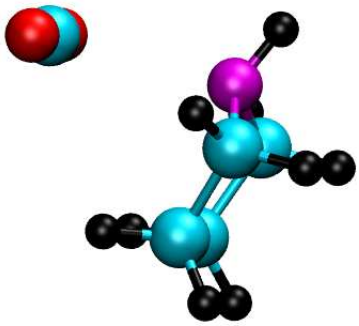

(a) pyrrolidine-CO_2 adduct

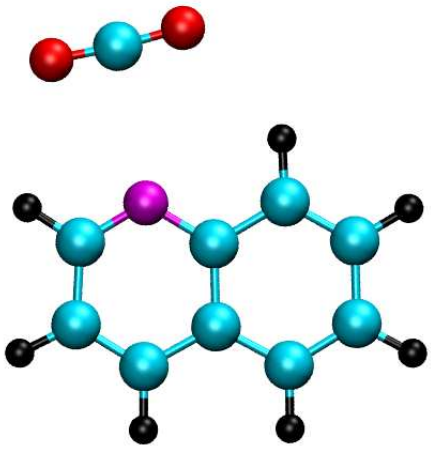

(b) quinoline-CO_2 adduct

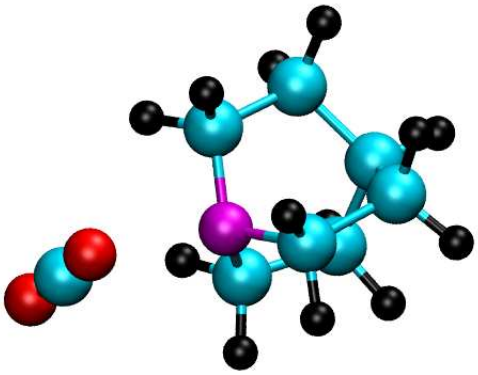

(c) quinuclidine-CO_2 adduct

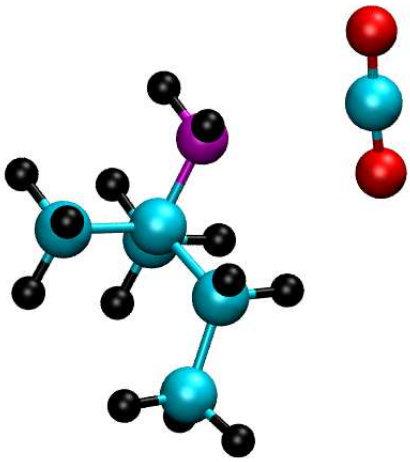

(d) tert-amylamine-CO_2 adduct

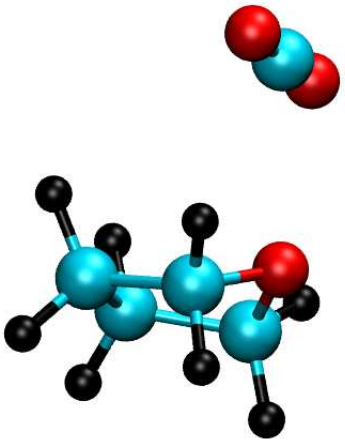

(e) tetrahydrofuran-CO_2 adduct

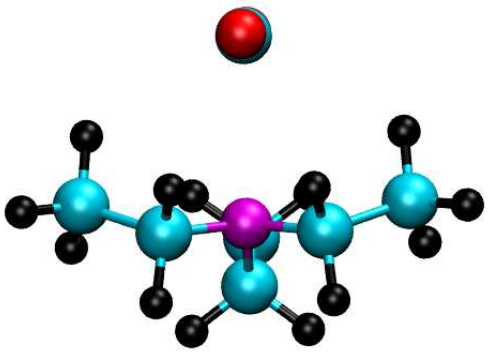

(f) triethylamine-CO_2 adduct

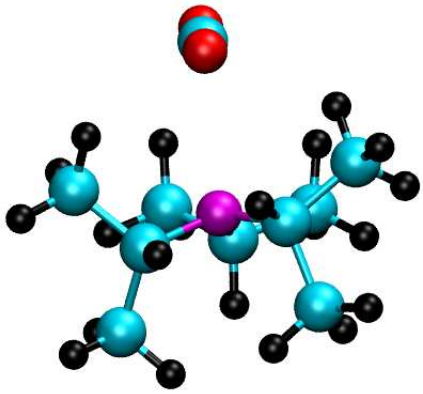

(a) triisopropylamine-CO_2adduct

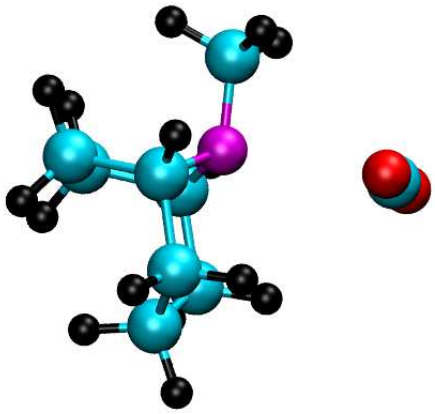

(b) tropane-CO_2 adduct

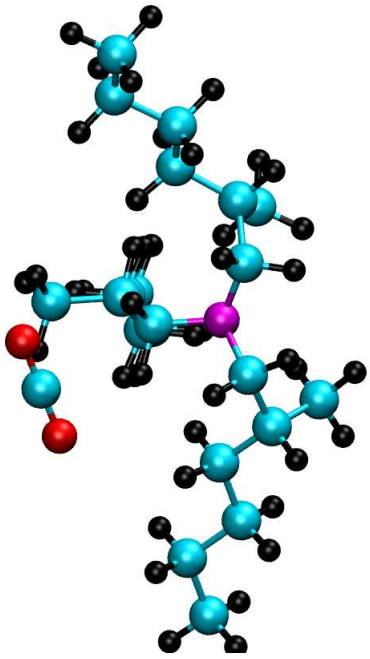

(c) tris-2-ethylhexylamine-CO_2 adduct

Table 3.1: Binding energy calculations

Serial No.	Base-CO_2 complex	BE_{nobsse} (kcal/mol)	BE_{bsse} (kcal/mol)	O-C-O angle (degrees)	Minimum distance (Å)
1	acetone	-3.96	-3.65	177.27	2.71
2	acetonitrile	-3.06	-2.82	178.59	2.84
3	aniline	-4.88	-4.29	177.86	3.32
4	diethylamine	-6.14	-5.54	175.49	2.72
5	diisopropylamine	-5.83	-5.22	175.85	2.78
6	dimethylethylamine	-6.32	-5.74	175.16	2.67
7	di-tert-amylamine	-6.09	-5.34	176.29	2.87
8	dimethylformamide	-4.71	4.25	177.14	2.69
9	dimethylsulfoxide	-6.72	-6.11	175.69	2.60
10	ethanol	-4.98	-4.58	177.29	2.62
11	ethanolamine	-5.34	4.85	176.57	2.62
12	ethylmethylamine	-6.06	-5.55	175.58	2.71
13	isopropylamine	-5.58	-5.00	175.81	2.75
14	isoquinoline	-5.56	-5.13	175.86	2.68
15	n-butylamine	-5.33	-4.77	175.83	2.76
16	piperidine	-5.94	-5.39	175.26	2.70
17	propylamine	-5.63	-5.05	175.77	2.75
18	pyridine	-5.48	-5.07	175.90	2.68
19	pyrrolidine	-6.57	-5.94	175.06	2.70
20	quinoline	-5.82	-5.29	176.09	2.74
21	quinuclidine	-6.22	-5.69	174.81	2.66
22	tert-amylamine	-5.59	-5.02	175.97	2.78
23	tetrahydrofuran	-9.52	-8.93	176.70	2.63
24	triethylamine	-6.30	-5.69	176.07	2.82
25	triisopropylamine	-5.06	-4.28	176.53	2.92
26	tropane	-6.28	-5.68	175.51	4.55
27	tris-2-ethylhexylamine	-5.78	-1.74	179.70	2.72

amine.[3] This behaviour can be explained by the increased number of +I groups attached to the donating atom. These groups being electron-donating in nature, increase the electron density on the donor atom. Thus, the Lewis basic character of the base increases and the binding energy of the CO_2-Lewis base complex increases. Another important factor affecting the relative basic strength (and corresponding binding energy) is the steric environment around the donating atom of the base. If there are more bulky, sterically hindering groups around the donor atom, it is more difficult for the base to donate electrons. This is the reason, precisely, for which, cyclic amines tend to donate electron pairs better than acyclic ones. There are no freely rotating large groups around the donor atom which can interfere with their ele

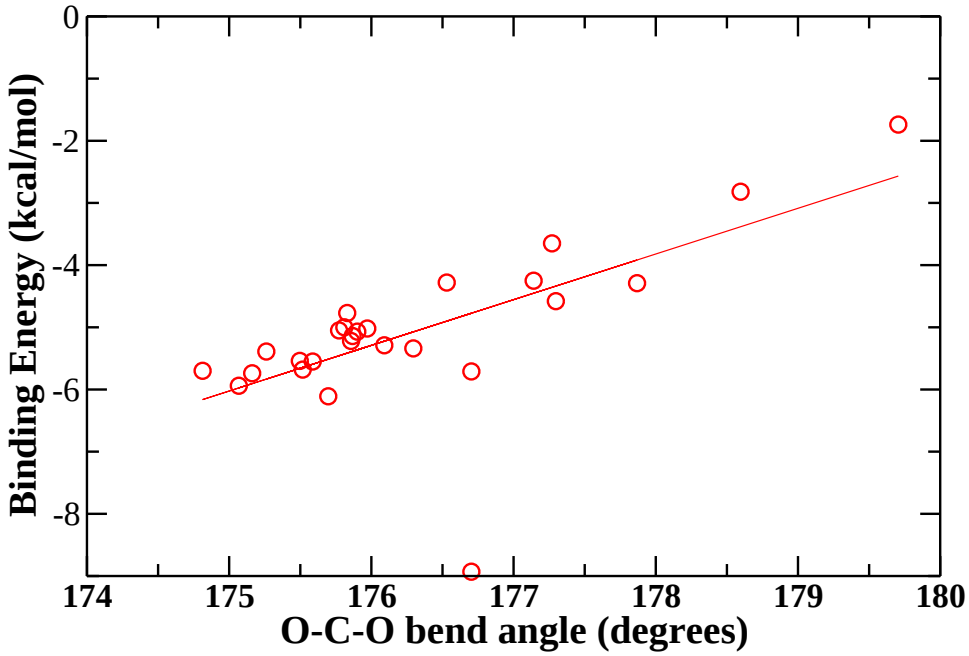

Figure 3.2: Variation of O-C-O angle of CO_2 with binding energy of Lewis base-CO_2 complex. Circles represent data point for each different complexes. The straight line is the best linear fit to the data.

With the variation of binding energy of the different Lewis bases with CO_2, intramolecular properties also change.[18] For example, if we measure the O-C-O angle

of CO_2 in the different complexes formed here, we will observe a pattern in the values of this angle. This plot of binding energy versus O-C-O angle of CO_2 is shown in figure 3.2. The plot clearly shows that complexes with stronger binding energy have greater deviation of the O-C-O angle of CO_2 from the actual 180°. The extent of distortion of O-C-O angle in CO_2 is found to be proportional to the binding energy of the Acid-base complex. Similar trends are observed for the non-nitrogenous bases, that is, bases with oxygen as the donor atom. Here also, we observe that cyclic bases have greater binding energy than the acyclic ones. The only cyclic base with oxygen atom as donor is Tetrahydrofuran which has a huge binding energy of -9.52 kcal/mol against dimethylsulfoxide which has the maximum binding energy of all the acyclic oxygen-donor bases, -6.72 kcal/mol. This behaviour can be attributed to the earlier mentioned steric factors. Another aspect arises if we now look into the behaviour among the acyclic bases, we find that dimethyl sulfoxide(DMSO) has the highest binding energy. This may be because, in this case, the electron density on the donor oxygen atom increases as the oxygen atom is directly attached to the sulfur atom which pushes the electron density towards the oxygen atom.

3.4 Conclusions

CO_2 is well known for its abundance and its role as a green house gas. Here, in this work, we have explored another interesting property of this molecule - its behaviour as a Lewis Acid. Since the carbon center is electron deficient in nature, it acts as a Lewis acid and accepts electron from other electron-rich species, namely, Lewis bases. This electron transfer from the base to acid leads to the formation of a Lewis acid-base adduct. The interaction between the two is not entirely electrostatic. However, the binding energy of this adduct gives us an idea about the stability of the adduct formed. It is believed that we can use this technique as a potential carbon dioxide sequestration method. This Lewis acid-base interaction can help to

remove CO_2 from the atmosphere and thus reduce its harmful effects.

Here, we have taken 27 potential Lewis bases, optimised their geometry to calculate the minimum energy structure. Then, we have calculated the binding energy of the complex formed by each of these bases with CO_2. All the possible orientations of approach of the CO_2 to the Lewis base has been explored. Further calculations are done only for the orientation with the minimum energy for each of the bases. We have also explored the change in the behaviour of the intramolecular property of CO_2 with the change in the binding energy of the complex.

Bibliography

[1] Lewis, G. *Valence and the Structure of Atoms and Molecules*; Monograph series; 1923.

[2] Mo, Y.; Gao, J. *J. Phys. Chem. A* **2001**, *105*, 6530–6536.

[3] Oliveri, I. P.; Maccarrone, G.; Di Bella, S. *J. Org. Chem.* **2011**, *76*, 8879–8884.

[4] Kazarian, S. G.; Vincent, M. F.; Bright, F. V.; Liotta, C. L.; Eckert, C. A. *J. Am. Chem. Soc.* **1996**, *118*, 1729–1736.

[5] Kollman, P. *J. Am. Chem. Soc.* **1977**, *99*, 4875–4894.

[6] Rochelle, G. T. *Science* **2009**, *325*, 1652–1654.

[7] Hounjet, L. J.; Caputo, C. B.; Stephan, D. W. *Angew. Chem. Int. Ed.* **2012**, *51*, 4714–4717.

[8] Sudik, A. C.; Millward, A. R.; Ockwig, N. W.; Ct, A. P.; Kim, J.; Yaghi, O. M. *J. Am. Chem. Soc.* **2005**, *127*, 7110–7118.

[9] ur Rahman, M. H.; Siaj, M.; Larachi, F. *Chemical Engineering and Processing: Process Intensification* **2010**, *49*, 313 – 322.

[10] Meredith, J. C.; Johnston, K. P.; Seminario, J. M.; Kazarian, S. G.; Eckert, C. A. *J. Phys. Chem.* **1996**, *100*, 10837–10848.

[11] Zhao, Y.; Truhlar, D. *Theo. Chem. Acc.* **2008**, *120*, 215–241.

[12] Hehre, W. J.; Ditchfield, R.; Pople, J. A. *J. Chem. Phys.* **1972**, *56*, 2257–2261.

[13] Clark, T.; Chandrasekhar, J.; Spitznagel, G. W.; Schleyer, P. V. R. *J. Comp. Chem.* **1983**, *4*, 294–301.

[14] Frisch, M. J.; Pople, J. A.; Binkley, J. S. *J. Chem. Phys.* **1984**, *80*, 3265–3269.

[15] Boys, S.; Bernardi, F. *Mol. Phys.* **1970**, *19*, 553–566.

[16] Frisch, M. J. et al. Gaussian 09 Revision D.01. Gaussian Inc. Wallingford CT 2009.

[17] Dennington, R.; Keith, T.; Millam, J. GaussView Version 5. Semichem Inc. Shawnee Mission KS 2009.

[18] Bhargava, B.; Balasubramanian, S. *Chem. Phys. Lett.* **2007**, *444*, 242 – 246.